

Signals for R -parity-violating Supersymmetry at a 500 GeV e^+e^- Collider

Dilip Kumar Ghosh

Department of Theoretical Physics, Tata Institute of Fundamental Research,
Homi Bhabha Road, Mumbai 400 005, India.

E-mail: dghosh@theory.tifr.res.in

Rohini M. Godbole

Centre for Theoretical Studies, Indian Institute of Science,
Bangalore 560 012, India.

E-mail: rohini@cts.iisc.ernet.in

Sreerup Raychaudhuri¹

Department of High Energy Physics, Tata Institute of Fundamental Research,
Homi Bhabha Road, Mumbai 400 005, India.

E-mail: sreerup@iris.hecr.tifr.res.in

Abstract

We investigate the production of charginos and neutralinos at a 500 GeV e^+e^- collider (NLC) and study their decays to the lightest neutralino, which then decays into multi-fermion final states through couplings which do not conserve R -parity. These couplings are assumed to affect only the decay of the lightest neutralino. Detailed analyses of the possible signals and backgrounds are performed for five selected points in the parameter space.

April 1999

¹ Address after May 1, 1999:

Department of Physics, Indian Institute of Technology, Kanpur 208 016, India.

1. Introduction: Non-conservation of R-Parity

The Minimal Supersymmetric Standard Model (MSSM) is currently the most popular option[1], for physics beyond the Standard Model (SM). A large part of contemporary effort in the search for new physics has, therefore, been devoted to searches for supersymmetry[2]. One of the cornerstones of most of these search strategies is the large missing energy and momentum signatures generated by an undetected neutralino, believed to be the lightest supersymmetric particle (LSP). This is constrained to be stable and weakly-interacting with matter because of conservation of a quantum number called R -parity, which is defined[3] to be

$$R = (-1)^{3B+L+2S} \quad (1)$$

where B, L and S represent, respectively, the baryon number, lepton number and intrinsic spin of the particle. This corresponds to the introduction, by hand, of a discrete Z_2 symmetry in the MSSM Lagrangian. Eq. (1) implies that $R = 1$ for all SM particles and $R = -1$ for all their supersymmetric partners (sparticles). In the SM, R -parity is trivially conserved, since each of B, L and S are separately conserved. The immediate consequence of R -parity conservation in the MSSM is that sparticles appear in pairs at each interaction vertex. Thus, each sparticle decays into another sparticle while, as mentioned above, the LSP cannot decay at all. Moreover the LSP must interact with matter through exchange of other (off-shell) sparticles. Since all the sparticles are known to be heavy, with masses of the order of the electroweak scale, the LSP's interaction with matter must be of weak strength; consequently, like the neutrino, it should escape most detectors. This leads to the missing energy and momentum signatures mentioned above. Such a stable particle is also a prime dark matter candidate[4] and, hence, must be neutral and weakly-interacting. The best candidate for the LSP in the MSSM is the lightest neutralino, and most experimental searches[2] for supersymmetry assume that this is indeed the case.

Since the conservation of R -parity plays such an important role in the search for supersymmetry, it is important to examine the reasons why it is believed to be a conserved quantum number. To see this, we note that the most general superpotential consistent with the gauge symmetry of the SM has the form[5]

$$\begin{aligned} \mathcal{W} = & \mu \hat{H}_2 \hat{H}_1 + h_{jk}^\ell \hat{H}_2 \hat{L}_j \hat{E}_k + h_{jk}^u \hat{H}_2 \hat{Q}_j \hat{U}_k + h_{jk}^d \hat{H}_1 \hat{Q}_j \hat{D}_k \\ & + \kappa_i \hat{L}_i \hat{H}_1 + \lambda_{ijk} \hat{L}_i \hat{L}_j \hat{E}_k + \lambda'_{ijk} \hat{L}_i \hat{Q}_j \hat{U}_k + \lambda''_{ijk} \hat{U}_i \hat{D}_j \hat{D}_k, \end{aligned} \quad (2)$$

where \hat{H}_1, \hat{H}_2 denote $SU(2)$ doublet Higgs superfields and \hat{L} (\hat{Q}) denote doublet lepton (quark) superfields containing the left-chiral leptons (quarks) as their fermion components. The $\hat{E}, \hat{U}, \hat{D}$ are the $SU(2)$ singlet lepton and quark superfields containing the right-chiral (charged) anti-leptons and anti-quarks, while i, j, k are flavour indices. In writing the above, we have dropped gauge indices, which ensure that (a) the λ_{ijk} are antisymmetric in i and j , and (b) the λ''_{ijk} are antisymmetric in j and k . The first three terms in the second line of Eq. (2) can be obtained simply by replacing, in the previous line, the Higgs superfield doublet \hat{H}_2 by any one of the three lepton superfield doublets \hat{L}_i , a procedure

which is made possible by the fact that these have the same gauge quantum numbers. The last term is a product of three $SU(2)$ singlets and clearly conserves charge.

It is immediately apparent that the first three terms in the second line of Eq. (2) violate lepton number (L), while the last violates baryon number (B). Both of these are conserved in the SM. Presence of *all* these terms can lead to catastrophically high rates for proton decay, which are certainly ruled out. In order to get a proton lifetime consistent with the current lower [6] bound ($\sim 10^{40}$ s), we would require [7, 8], typically $\lambda'\lambda'' \lesssim 10^{-26}$. Now this is highly unnatural, unless one or both of λ' and λ'' happen to be identically zero. The imposition of R -parity conservation ensures this by forbidding *all* the terms in the second line of Eq. (2) and, therefore, constitutes a simple solution to the problem of fast proton decay in supersymmetric models.

Though the R -parity argument is rather attractive, it was pointed out long ago [5] that, as a solution to the proton decay problem, it constrains the model more than what is really necessary. To ensure vanishing contributions to proton decay, it is quite adequate to ensure that *one* of the couplings in the product $\lambda'\lambda''$ vanishes — not both. For example [8], if we demand baryon number conservation, and allow lepton number to be violated, then the λ'' terms vanish and the proton remains stable, but R -parity is no longer a good symmetry because of the lepton-number-violating terms in the superpotential. Conversely, if we demand lepton number conservation, then the first three terms in the second line of Eq. (2) vanish, but the last term, which violates baryon number, remains as a source of R -parity non-conservation. We note, in this context, that the imposition of baryon number conservation is somewhat better motivated from theoretical considerations [9] than its counterpart in the lepton sector.

It is at once obvious that if we allow for either lepton number or baryon number to be violated in supersymmetric interactions, then it should be possible to see some effects in low-energy interactions or in precision electroweak measurements. Since these have not been seen to date, it has been shown that all R -parity-violating effects at low and electroweak scale energies must be rather small, and, therefore, R -parity does survive, at least as an approximate symmetry. However, smallness of these deviations from the SM is partly ensured by the fact that they must occur through the exchange of heavy virtual sfermions and are, thus, naturally suppressed. Despite this, current measurements are still precise enough to constrain the R -parity-violating couplings to be rather small, unless, indeed, the sfermions are very heavy (~ 1 TeV or more). In fact, there exists a whole series of upper bounds on these couplings [10] and some of these are updated regularly in the literature [11, 12].

The situation changes rather dramatically when one considers signals for supersymmetry at high energy colliders. If we allow for the non-conservation of R -parity, then we have the following possibilities:

- The LSP need no longer be stable. It is possible, given a specific structure for the R -parity-non-conserving sector, to write down its decay modes.
- The lightest neutralino need not be the LSP since the arguments in favour of this are based on the LSP being stable and forming the major component of cosmic dark matter.

An unstable LSP thus leads to one of the less attractive features of supersymmetric models without R -parity conservation, which is the loss of an excellent dark matter candidate. However, one can always assume that there are other candidates such as, for example, invisible axions, machos or wimps. In fact, though the existence of certain amounts of galactic dark matter is undoubted, it might be relevant to point out that the need for cosmic dark matter is itself based on a theoretical prejudice that the universe should be closed. The cosmological argument for conservation of R -parity, though plausible, should not be regarded as a clinching one.

The above discussion makes it clear that there is no compelling phenomenological reason for the introduction of R -parity as a discrete symmetry in the MSSM. If, indeed, it is conserved, as the smallness of upper bounds on R -parity-violating couplings may lead us to suspect, there must be a deep and hitherto unknown theoretical reason for the corresponding discrete symmetry to be obeyed. In fact, even the smallness of the couplings is a constraint which is valid[10] only if the sfermions are rather light. For heavy sfermions, it is quite possible for R -parity violation — in either of its avatars as lepton number or baryon number violation — to be quite significant. If this turns out to be the case, supersymmetric models with R -parity violation could become a subject of considerable interest.

It is useful, at this stage, to note that the κ_i terms can, in principle, be removed by a redefinition of the lepton doublets \hat{L}_i which leads to absorption of the κ_i in the λ, λ' couplings and in the parameters of the scalar potential of the model. However, these would then reappear at a different energy scale[13]. Bilinear terms could also lead to a possible vacuum expectation value (VEV) for the sneutrino(s) and mixing of (a) charged leptons with charginos, (b) sleptons with charged Higgs bosons, (c) neutrinos with neutralinos and (d) sneutrinos with neutral Higgs bosons. The phenomenological consequences of a sneutrino VEV and lepton-number-violating mixing have been discussed in the literature[14], but will not be pursued further in this article. We are, therefore, making the assumption that the κ_i terms are small.

Having re-examined the reasons for assuming R -parity conservation and hence the existence of a stable LSP giving rise to missing energy and momentum signals at colliders, we thus come to the conclusion that this is merely *one* of the possible supersymmetric scenarios and it is certainly necessary to make a re-evaluation of supersymmetry signals in the case when the LSP *can* decay. The implications of R -parity violation for sparticle searches have been considered both by theorists and experimentalists. It was found [15] that the limits on squark and gluino masses from the Tevatron data in the presence of R -parity violation are comparable to those obtained assuming R -parity conservation. Like-sign dileptons can also be used quite effectively[15, 16] for such searches at the Tevatron. Prospects for sparticle searches in the presence of R -parity violation at future pp colliders like LHC are also fairly bright[11]. It was also pointed out [17] that chargino and/or neutralino production at LEP would be a good place to look for signals for supersymmetry with broken R -parity.

Studies of the above nature, neglected until a short time ago, have now been included in the agenda of most of the major running experimental facilities, such as those at LEP-2 and the Tevatron. The four experimental collaborations at LEP have made separate studies [18] of signals for R -parity-violating supersymmetry and we take note of their bounds in our analysis. Similar bounds exist from the Tevatron

Run I data[19]. However, we must note that LEP is already near the end of its kinematic reach, and unless, indeed, supersymmetric particles are lying just around the corner, waiting to be discovered, it is unlikely that we will obtain anything more than improved bounds from the present and future runs of LEP. Better hopes may be placed on the Run II of the Tevatron and the TeV-33 run², and, of course, the LHC, but it is really to the clean environment of a 500 GeV linear e^+e^- collider, such as the planned Next Linear Collider (NLC), that we must look[20, 21] if we wish to complement the information from hadron colliders and further help find unambiguous signals for low-energy supersymmetry³. The present work is devoted therefore, to a preliminary study of the production of charginos and neutralinos at a 500 GeV linear e^+e^- collider, and their decays in the presence of R -parity-violating couplings. Signal studies for the R -parity-conserving option may be found in the literature [22, 23]. What really distinguishes our analysis from similar studies at LEP-2 is the higher collision energy, which opens up the possibility of copious production of the *heavier* chargino and neutralino states. Their cascade decays can then add to the signals, but also introduce additional complications because of the multiplicity of possible final states. We present here a first attempt to sort out these possibilities and obtain distinguishable signals. It turns out that the heavier chargino/neutralino states, though they make the analysis complicated, are ultimately more of a help than a hindrance in signatures deciphering for R -parity-violating supersymmetry from the backgrounds.

The particular scenario which is discussed in this article is the so-called *weak limit* of R -parity violation [24], where the R -parity-violating couplings are considerably smaller than the gauge couplings. This is partly motivated by the fact that current upper bounds on the R -parity-violating couplings are typically an order of magnitude below the gauge couplings for sfermion masses near the electroweak symmetry-breaking scale[11]. However, this is not a particularly compelling argument, since we have just argued the case for heavy sfermions relaxing these bounds. The current choice of scenario should, therefore, be regarded as motivated principally by a requirement of *minimal deviation* from the R -parity-conserving model. As a result, most production and decay processes in this analysis will take place along the lines expected in the MSSM in the R -parity-conserving case. Though it is no longer an absolute necessity (irrespective of the strength of the couplings), the LSP will still be assumed to be the lightest neutralino, and its decays will form the chief point of departure of our study from earlier ones involving a stable and invisible LSP. Our study is thus, in a sense, complementary to the work of Refs. [25, 21, 26], who discuss processes at e^+e^- colliders where the R -parity violation takes place directly at the production vertices. These studies require large R -parity-violating couplings, while the one undertaken here assumes small couplings.

Though we assume the R -parity-violating couplings to be much smaller than the gauge couplings, we still require the couplings relevant for decay of the LSP to be large enough to ensure that it decays within the detector. This point is, however, somewhat academic, since, even with couplings one or two orders of magnitude below the current upper bound, the LSP will decay (for all practical purposes) at the interaction point itself and thus will not even exhibit displaced vertices.

²Should it happen

³Assuming that the sparticle spectrum is not too heavy for such a machine.

The plan of this article is as follows. A large part of the material that goes into a discussion of chargino and neutralino production and decay in the MSSM is already available in the literature. In the following section, we make some general remarks concerning processes which lead to the production of a pair of charginos or neutralinos at an e^+e^- collider and present contour plots in the parameter space showing the importance of each channel at NLC energies. We also explain our choice of the five points in the parameter space where a detailed analysis has been done. The results of this section are relevant even if R -parity is assumed to be conserved. In section 3 we discuss the decay of the LSP into multi-fermion channels through R -parity-violating couplings and then go on to consider decay modes of the heavier charginos and neutralinos to the LSP (which are again of general interest). Sections 4, 5 and 6 are devoted to a study of the different signals predicted in the case of $\lambda, \lambda', \lambda''$ couplings respectively as well as the relevant backgrounds. Our results are summed-up in Section 7. In the Appendices, we present detailed formulae for the decay of the LSP and exhibit typical results which might be of interest if the NLC has a $\sqrt{s} = 350$ GeV centre-of-mass stage. We also discuss some details of the background studies.

2. Chargino and Neutralino Pair-production in e^+e^- Collisions

Computing production cross sections for charginos and neutralinos in the MSSM is a complex business. There are no R -parity-violating contributions to the production mechanism in the weak limit. Nevertheless, it is difficult to make remarks which hold in the general case. The cross sections depend critically on the masses and mixing angles of charginos and neutralinos, which, in turn, depend on the parameters $M_1, M_2, \mu, \tan \beta$ of which the mass matrices are made up. In this article, we assume gaugino mass unification at a high scale, which means that M_1 and M_2 are linearly related by:

$$M_1 = \frac{5}{3} \tan^2 \theta_W M_2 . \quad (3)$$

Thus, the free parameters in question are $M_2, \mu, \tan \beta$ and, of course, the masses of the left and right selectrons. The mass of the electron sneutrino is not a free parameter, being related to the mass of the left selectron by the $SU(2)$ -breaking relation

$$m_{e_L}^2 = m_{\nu_e}^2 - \frac{1}{2} M_W^2 \cos 2\beta . \quad (4)$$

The free parameters $M_2, \mu, \tan \beta$ decide the masses as well as the mixing angles of the charginos and neutralinos. Apart from the mixing angles, which go into the Feynman rules, the other major question in determining the production cross sections is that of kinematics. For a centre-of-mass energy of 500 GeV, it is rather difficult to produce pairs of the heavier charginos $\tilde{\chi}_2^\pm$ or the heavier neutralinos $\tilde{\chi}_3^0$ and $\tilde{\chi}_4^0$, except in narrow regions of the parameter space where both the charginos or all the neutralinos are light. However, the lighter states, $\tilde{\chi}_1^\pm, \tilde{\chi}_1^0, \tilde{\chi}_2^0$, can be freely produced.

Given the large number of unknown parameters and the variety of scenarios for R -parity violation, it is not practical to present a detailed analysis of the signals over the *entire* parameter space. We have

chosen, for detailed analysis, five particular points in the MSSM parameter space which are allowed by the current LEP data and where the masses and mixings of the gaugino and higgsino states have different, but typical, features⁴. These five points are

- (A) $M_2 = 100$ GeV, $\mu = -200$ GeV, $\tan\beta = 2$, $M_{\tilde{e}_L} = M_{\tilde{e}_R} = 150$ GeV,
- (B) $M_2 = 150$ GeV, $\mu = +150$ GeV, $\tan\beta = 20$, $M_{\tilde{e}_L} = M_{\tilde{e}_R} = 150$ GeV,
- (C) $M_2 = 150$ GeV, $\mu = +250$ GeV, $\tan\beta = 2$, $M_{\tilde{e}_L} = M_{\tilde{e}_R} = 150$ GeV,
- (D) $M_2 = 150$ GeV, $\mu = -250$ GeV, $\tan\beta = 20$, $M_{\tilde{e}_L} = M_{\tilde{e}_R} = 200$ GeV,
- (E) $M_2 = 200$ GeV, $\mu = -250$ GeV, $\tan\beta = 20$, $M_{\tilde{e}_L} = M_{\tilde{e}_R} = 200$ GeV.

Apart from the obvious fact that round numbers have been used for M_2 and μ , we have concentrated on two values of $\tan\beta$, namely 2 and 20. The lower value corresponds to what is likely to be the lower bound[28] on $\tan\beta$ from non-observation of the lightest Higgs boson when LEP-2 has finished its run, while the upper value is a reasonably high one, though not quite the highest allowed by the present constraints. Throughout this analysis, the soft supersymmetry-breaking squark masses have been set to the common value 500 GeV, and the trilinear couplings to $A_t = A_b = A_\tau = 0$.

Point	Particle	mass	wino \tilde{W}^\pm	higgsino \tilde{H}^\pm
A	$(\tilde{\chi}_1^\pm)_L$	112.1 GeV	0.0 %	100.0 %
	$(\tilde{\chi}_1^\pm)_R$		20.5 %	79.5 %
	$(\tilde{\chi}_2^\pm)_L$	224.3 GeV	100.0 %	0.0 %
	$(\tilde{\chi}_2^\pm)_R$		79.5 %	20.5 %
B	$(\tilde{\chi}_1^\pm)_L$	99.9 GeV	33.1 %	66.9 %
	$(\tilde{\chi}_1^\pm)_R$		66.9 %	33.1 %
	$(\tilde{\chi}_2^\pm)_L$	218.8 GeV	66.9 %	33.1 %
	$(\tilde{\chi}_2^\pm)_R$		33.1 %	66.9 %
C	$(\tilde{\chi}_1^\pm)_L$	110.5 GeV	17.5 %	82.5 %
	$(\tilde{\chi}_1^\pm)_R$		28.0 %	72.0 %
	$(\tilde{\chi}_2^\pm)_L$	292.7 GeV	82.5 %	17.5 %
	$(\tilde{\chi}_2^\pm)_R$		72.0 %	28.0 %
D	$(\tilde{\chi}_1^\pm)_L$	135.2 GeV	6.9 %	93.1 %
	$(\tilde{\chi}_1^\pm)_R$		27.8 %	72.2 %
	$(\tilde{\chi}_2^\pm)_L$	282.1 GeV	93.1 %	6.9 %
	$(\tilde{\chi}_2^\pm)_R$		72.2 %	27.8 %
E	$(\tilde{\chi}_1^\pm)_L$	173.4 GeV	18.0 %	82.0 %
	$(\tilde{\chi}_1^\pm)_R$		41.2 %	58.8 %
	$(\tilde{\chi}_2^\pm)_L$	292.1 GeV	82.0 %	18.0 %
	$(\tilde{\chi}_2^\pm)_R$		58.8 %	41.2 %

Table 1. *Masses and compositions of the two charginos at the five selected points (see text).*

The masses and compositions of the charginos at these points are given in Table 1. It is at once obvious that at point (A), the left-handed charginos are pure states, while the right-handed charginos are mixed states. At the other points both left- and right-handed charginos are mixed states, though

⁴The inspiration for this comes from the procedure followed for the constrained MSSM at Snowmass[27], though we have not taken their precise values

point (D) is close to a pure state. The mass of the lighter chargino varies from about 100 GeV for point (B) to near the top quark mass for point (E). We thus get a span of most of the different possibilities. Note that $\tilde{\chi}_2^\pm$ has mass above 200 GeV (and $M_{\tilde{e}_L} > M_{\tilde{\chi}_1^\pm}$) for all the five points.

Charginos will be pair-produced in e^+e^- collisions through the three Feynman diagrams of Fig. 1(a). Except for the photon-exchange diagram, the others can result in production of a pair of dissimilar charginos (provided it is kinematically allowed). These diagrams have been evaluated before and formulae are readily available in the literature[29]. In this section, we confine ourselves to some general remarks on the production process.

Noting (see, Table 1) that the chargino is a linear combination of a wino and a charged higgsino state, and that its couplings are obtained by supersymmetrizing the corresponding gauge and Yukawa couplings respectively, it is obvious that the t -channel sneutrino-exchange diagram makes a significant contribution only if the charginos $\tilde{\chi}_1^\pm$ and $\tilde{\chi}_2^\pm$ have substantial wino components, since the coupling of the higgsino components to electrons are suppressed by m_e/M_W ($\sim 10^{-6}$). In such regions of the parameter space, however, the same t -channel diagram interferes destructively with the others, leading to a well-known dip in the cross section when it is plotted as a function of the mass of the exchanged electron sneutrino.

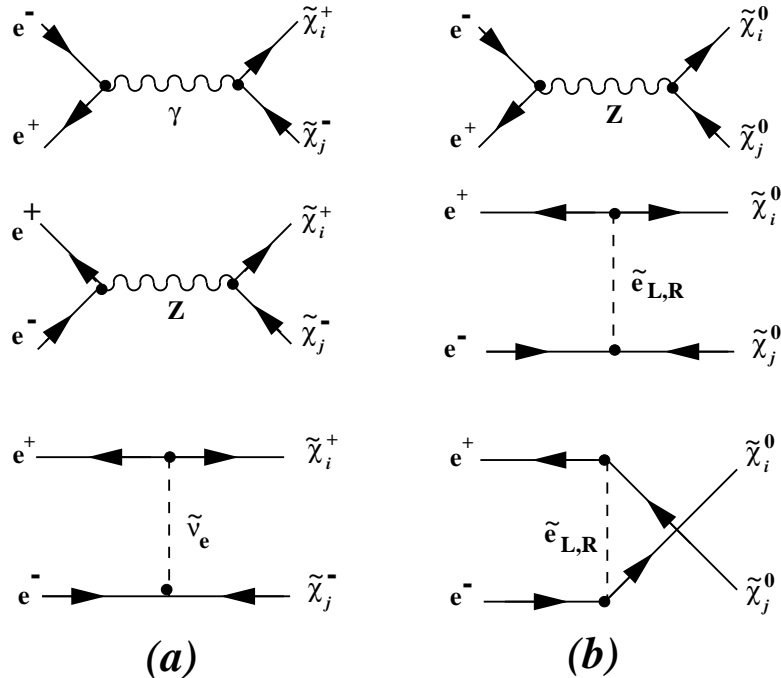


Figure 1. Feynman diagrams contributing to the processes (a) $e^+e^- \rightarrow \tilde{\chi}_i^+ \tilde{\chi}_j^-$ and (b) $e^+e^- \rightarrow \tilde{\chi}_i^0 \tilde{\chi}_j^0$ in the MSSM.

In Fig. 2(A) and 2(B), we plot the cross sections for production of

$$\tilde{\chi}_1^+ \tilde{\chi}_1^-, \quad \tilde{\chi}_1^\pm \tilde{\chi}_2^\mp, \quad \tilde{\chi}_2^+ \tilde{\chi}_2^-,$$

as functions of the mass of the left selectron, which is related to the mass of the electron-sneutrino by

Eq. (4). Fig. 2(A) corresponds to the point (A) and Fig. 2(B) corresponds to the point (B) in the list of selected points in the parameter space. One must remember that the cross section for production of a pair of dissimilar charginos should be multiplied by a combinatoric factor of 2. It is now obvious that the cross section for the production of a pair of lighter charginos $\tilde{\chi}_1^+ \tilde{\chi}_1^-$ is much larger than similar cross sections for production of the heavier chargino states. Cross-sections for production of one light and one heavy state get heavily suppressed as the sneutrino mass grows larger and thus may be seen to originate almost entirely from the t -channel sneutrino exchange. As a result, the suppression is stronger in case (A) where the charginos are pure states. Fig. 2(B), however, shows the characteristic dip in production of $\tilde{\chi}_2^+ \tilde{\chi}_2^-$ due to s and t -channel interference. It is clear therefore, that the bulk of the signal will originate from production of a pair of lighter charginos.

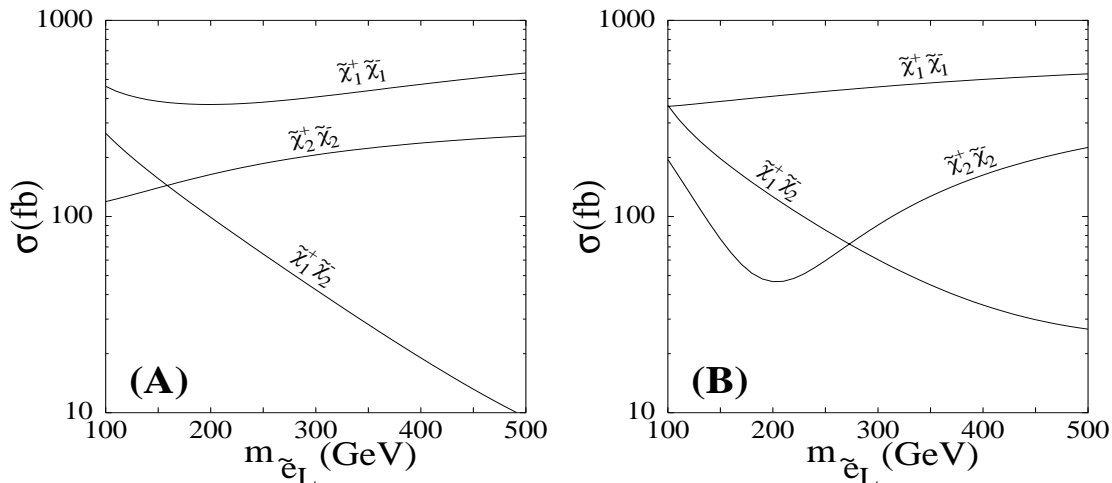


Figure 2. Cross-sections for chargino pair production with parameter choices (A) and (B) as given in the text. Cross sections for dissimilar charginos should be multiplied by a factor of 2.

Neutralinos will also be pair-produced in e^+e^- collisions through the Feynman diagrams given in Fig. 1(b). There is (naturally) no photon-exchange diagram, but now there is a u -channel as well as a t -channel diagram with selectron exchange to which both left and right selectrons can contribute. This is because of the Majorana nature of the neutralinos. The final amplitude is thus the coherent sum of five diagrams with the signs chosen carefully so that t - and u -channels add to the s -channel diagram with opposite signs because of odd and even numbers of permutations arising in the Wick contractions. All the diagrams can result in the production of similar or dissimilar neutralinos, so that we can have ten distinct final states. As in the case of charginos, these diagrams have been evaluated before and formulae are readily available in the literature[29].

The process $e^+e^- \rightarrow \tilde{\chi}_i^0 \tilde{\chi}_j^0$, like the analogous process with charginos, depends crucially on the composition of the neutralino(s) involved. As in the case of charginos, we may safely conclude that the higgsino components of the neutralino are irrelevant. For right selectron exchange, in fact, the wino component is also irrelevant and the electron-left selectron coupling depends solely on the bino component. Thus, the contributions of the t and u -channel diagrams in Fig. 1(b) require substantial gaugino components of the relevant neutralinos. For the s -channel diagram, it is a different story.

The $Z\tilde{\chi}_i^0\tilde{\chi}_j^0$ coupling arises from supersymmetrization of the $ZH_1^0H_2^0$ coupling and thus a significant contribution can arise only if there is a significant higgsino component in each of the two neutralinos. Fortunately, the structure of the neutralino mass matrix in the higgsino sector is such[1] that a higgsino-dominated neutralino must be a near-equal mixture of the two higgsino states, so that this scenario covers a greater part of the parameter space than what might naively be expected.

Point	Particle	mass	photino $\tilde{\gamma}$	zino \tilde{Z}	higgsinos $\tilde{H}_1^0, \tilde{H}_2^0$
A	$\tilde{\chi}_1^0$	54.3 GeV	86.9 %	11.3 %	1.8 %
	$\tilde{\chi}_2^0$	111.9 GeV	12.9 %	73.5 %	13.6 %
	$\tilde{\chi}_3^0$	208.5 GeV	0.2 %	7.9 %	91.9 %
	$\tilde{\chi}_4^0$	224.4 GeV	0.0 %	7.3 %	92.7 %
B	$\tilde{\chi}_1^0$	63.4 GeV	40.4 %	35.1 %	24.5 %
	$\tilde{\chi}_2^0$	107.3 GeV	56.5 %	12.1 %	31.4 %
	$\tilde{\chi}_3^0$	163.6 GeV	0.1 %	4.6 %	95.3 %
	$\tilde{\chi}_4^0$	218.3 GeV	3.0 %	48.1 %	48.9 %
C	$\tilde{\chi}_1^0$	62.5 GeV	46.9 %	43.4 %	9.7 %
	$\tilde{\chi}_2^0$	117.7 GeV	52.6 %	33.0 %	14.4 %
	$\tilde{\chi}_3^0$	252.3 GeV	0.0 %	0.6 %	99.4 %
	$\tilde{\chi}_4^0$	297.6 GeV	0.5 %	22.9 %	76.5 %
D	$\tilde{\chi}_1^0$	73.7 GeV	70.0 %	25.7 %	4.3 %
	$\tilde{\chi}_2^0$	135.2 GeV	29.5 %	53.6 %	17.0 %
	$\tilde{\chi}_3^0$	262.0 GeV	0.0 %	3.0 %	97.0 %
	$\tilde{\chi}_4^0$	278.6 GeV	0.5 %	17.7 %	81.8 %
E	$\tilde{\chi}_1^0$	97.7 GeV	68.5 %	26.3 %	5.3 %
	$\tilde{\chi}_2^0$	173.6 GeV	29.6 %	42.1 %	28.3 %
	$\tilde{\chi}_3^0$	260.8 GeV	0.0 %	2.5 %	97.5 %
	$\tilde{\chi}_4^0$	290.1 GeV	1.9 %	29.2 %	68.9 %

Table 2. Masses and compositions of neutralinos at the five selected points (see text). In the last column, we give the combination of the two neutral higgsinos.

Following the same procedure as for charginos, we detail in Table 2 the composition of the neutralinos at the five selected points. At all the points, the LSP is gaugino-dominated, being mainly photino in cases (A), (D) and (E) and having substantial zino components in cases (B)–(E). It has a substantial higgsino component only in case (B). The higher neutralinos $\tilde{\chi}_3^0$ and $\tilde{\chi}_4^0$ have none or very small photino components, in all the cases. The $\tilde{\chi}_3^0$ turns out to be mostly higgsino-dominated, while the $\tilde{\chi}_4^0$, though principally higgsino, has substantial zino components as well.

In Fig. 3(a – f), we plot the cross sections for production of $\tilde{\chi}_i^0\tilde{\chi}_j^0$ as functions of (a, b) the mass of the left selectron, when the mass of the right selectron is set to 150 GeV; (c, d) the mass of the right selectron, when the mass of the left selectron is set to 150 GeV, and (e, f) the common mass of the selectron in the case when left and right selectrons are degenerate. Only the combinations

$$\tilde{\chi}_1^0\tilde{\chi}_1^0, \quad \tilde{\chi}_1^0\tilde{\chi}_2^0, \quad \tilde{\chi}_1^0\tilde{\chi}_3^0, \quad \tilde{\chi}_1^0\tilde{\chi}_4^0, \quad \tilde{\chi}_2^0\tilde{\chi}_2^0, \quad \tilde{\chi}_2^0\tilde{\chi}_3^0, \quad \tilde{\chi}_2^0\tilde{\chi}_4^0$$

have been shown. The graphs on the left, namely (a, c, e), correspond to the point (A), while the graphs on the right, namely (b, d, f), correspond to the point (C). One must also remember that cross sections with dissimilar neutralinos carry an extra combinatoric factor of 2, while cross sections with identical neutralinos already carry a factor of half because of quantum statistics. It is now obvious from the figure, that the production of $\tilde{\chi}_1^0$ and $\tilde{\chi}_2^0$, either as similar or dissimilar pairs, exceeds production of the heavier states $\tilde{\chi}_3^0, \tilde{\chi}_4^0$ roughly by an order of magnitude⁵. This is an important result, and it will enable us, in the next section, to simplify search strategies considerably.

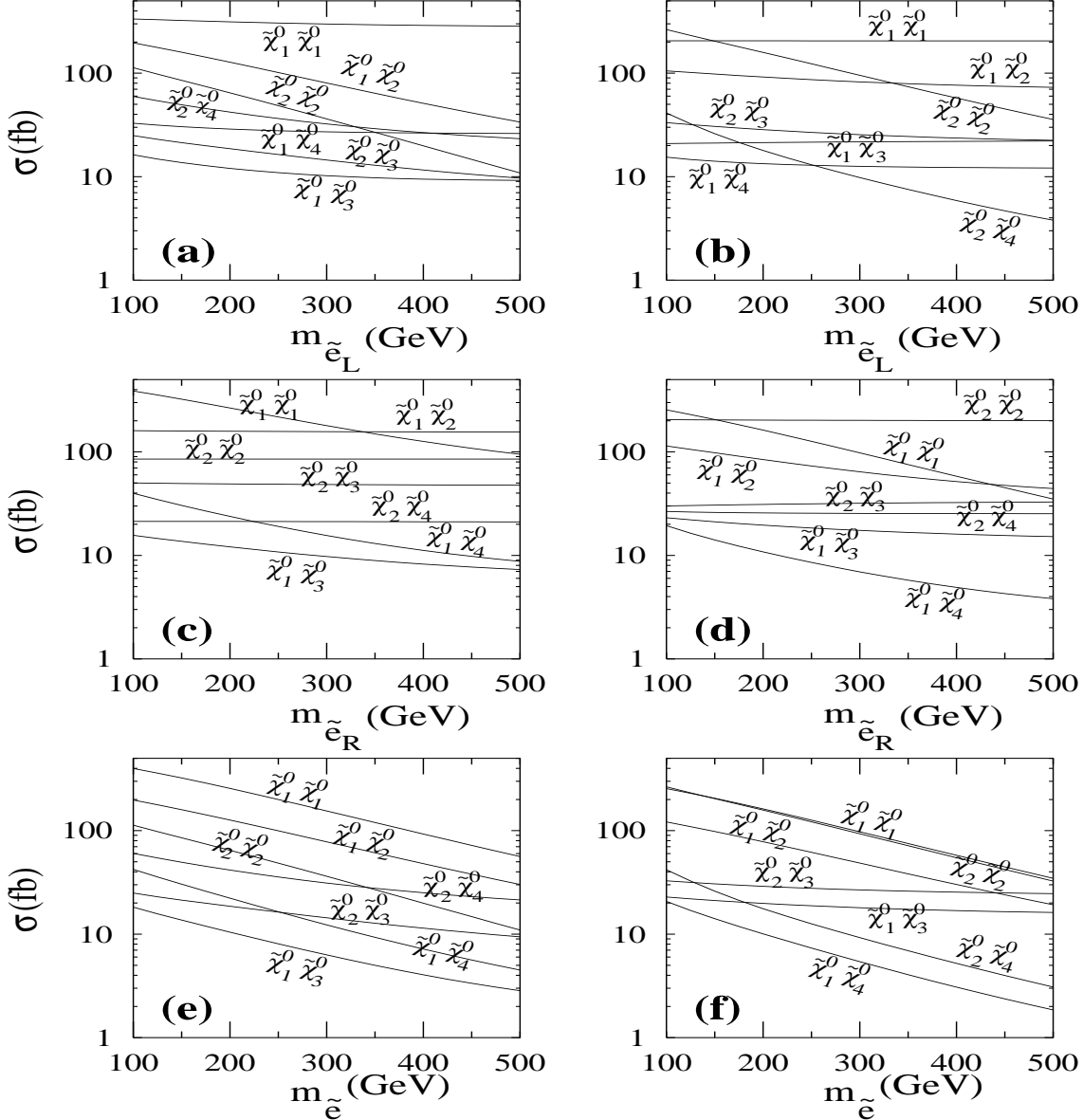


Figure 3. Cross-sections for neutralino pair production at the points (A) and (C). Cross sections for dissimilar neutralinos should be multiplied by 2. For (e, f) left and right selectrons are degenerate.

⁵Unless the selectron is very heavy; in this case, all the cross sections are small anyway.

The illustrative results in Figs. 2 and 3 are, of course, obtained by considering three of the selected points in the parameter space. It is now relevant to ask whether we can generalize the principal conclusion — that it is only important to consider production modes of the $\tilde{\chi}_1^0$, $\tilde{\chi}_2^0$ and $\tilde{\chi}_1^\pm$ to observe signals at a 500 GeV machine — to the entire parameter space. Part of the answer is given by kinematics: the current bounds[18] on the $\tilde{\chi}_1^\pm$ mass from LEP-2 force the heavier states $\tilde{\chi}_3^0$, $\tilde{\chi}_4^0$ and $\tilde{\chi}_2^\pm$ to have masses fairly close to the kinematic reach of a 500 GeV machine. This is illustrated in Fig. 4, where we have shown scatter plots of the heavier chargino and neutralino masses as M_2 varies over the range 0 to 600 GeV, μ varies from -600 to 600 GeV and $\tan\beta$ varies from 1.5 to 50. Clearly, when there is no experimental constraint on the MSSM, all the states are well within the kinematic reach of a 500 GeV machine (which corresponds to the 250 GeV box). Imposition of the LEP-2 constraint $\tilde{\chi}_1^\pm > 91$ GeV immediately drives the heaviest chargino and neutralino states (practically) out of the box, while the intermediate states $\tilde{\chi}_2^0$ and $\tilde{\chi}_3^0$ are driven to heavier, but not kinematically inaccessible values. One can therefore, safely write off the $\tilde{\chi}_4^0$ and $\tilde{\chi}_2^\pm$ states. It only remains, therefore, to ask whether it is relevant to include the $\tilde{\chi}_3^0$ in our analysis. For this, the *dynamics* of the production cross section(s) must now be considered.

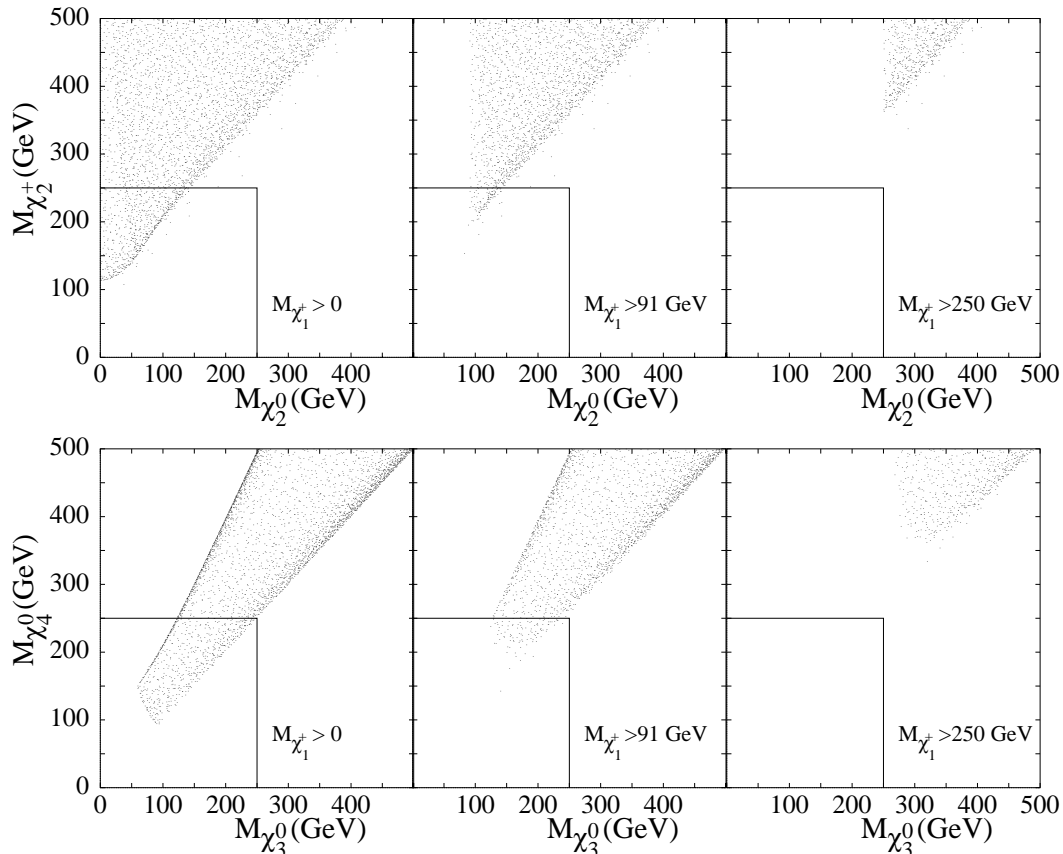


Figure 4. Scatter plots for higher chargino and neutralino masses in the MSSM. The ranges of variation of the parameters are given in the text. The box represents the kinematic reach of a 500 GeV machine.

Before we discuss this, however, it is interesting to look at the graphs on the extreme right of Fig. 4.

These would correspond to the (disappointing) situation when a 500 GeV e^+e^- collider has completed its run without finding any evidence of supersymmetry and has been able to push the lower bound on the mass of the lighter chargino to ~ 250 GeV. It is likely that the machine would then be upgraded to 1 TeV in energy[23], kinematic limits for which correspond to the outer boxes in the figure. In this case, we see that the same pattern repeats itself, with the heavier states being pushed almost out of the picture. Thus the broad conclusions of this work would still hold in the newer context and almost identical studies can be made.

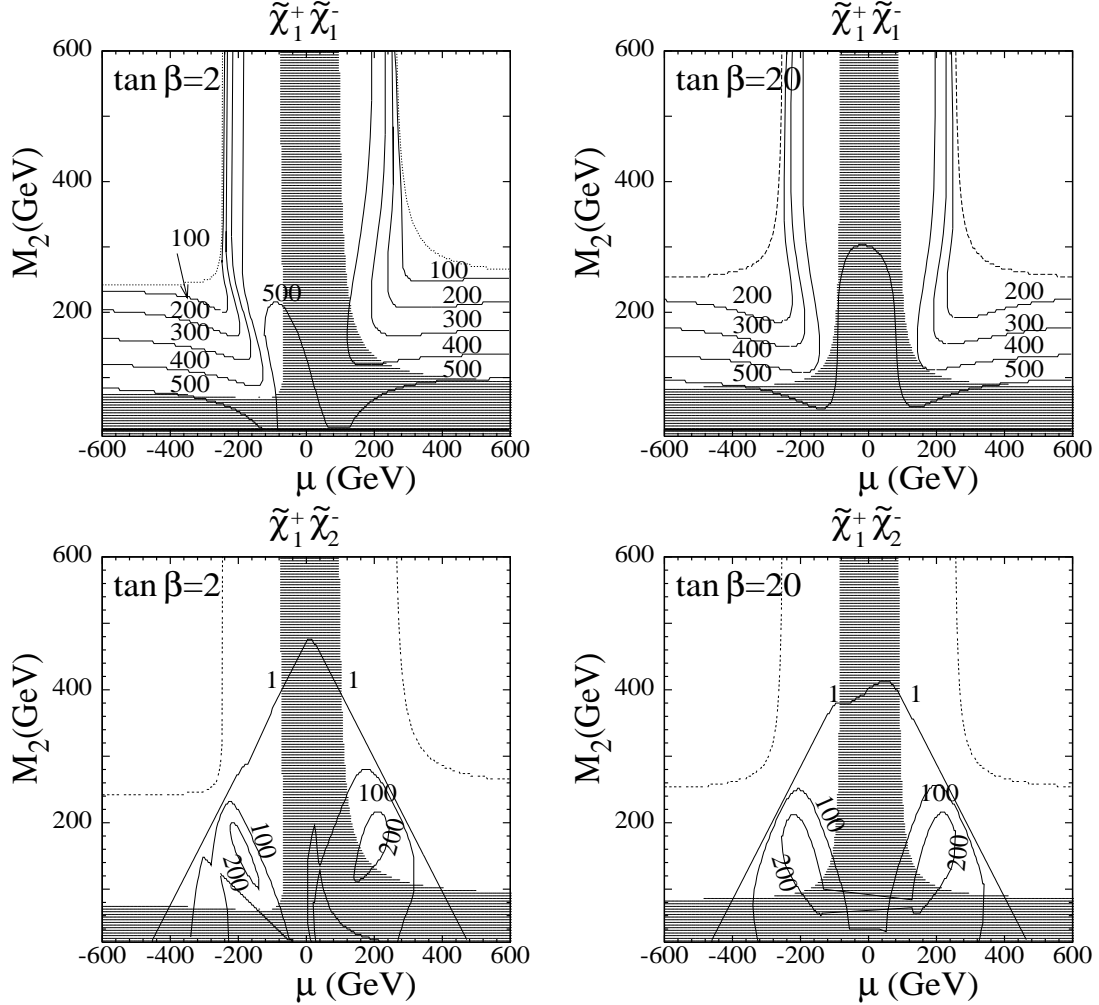


Figure 5. Contours of cross section (marked in fb) for production at the NLC of a pair of charginos for $\tan \beta = 2$ and 20 and $M_{\tilde{e}_L} = M_{\tilde{e}_R} = 150$ GeV.

In Fig. 5, we present contours for the cross section (in fb) for the production of $\tilde{\chi}_1^+ \tilde{\chi}_1^-$ and $\tilde{\chi}_1^+ \tilde{\chi}_2^-$ final states in the (M_2, μ) plane for two values of $\tan \beta$, namely, $\tan \beta = 2$ for the plots on the left and $\tan \beta = 20$ for the plots on the right. The left selectron is assumed to have a mass of 150 GeV. It is clear from the figure that production of even a single heavy chargino state leads to considerable reduction in the cross section. Even so, the cross section is relatively large in pockets close to the LEP-excluded region, where it is about 15–20% of the cross section for production of a pair of lighter charginos. As

most of the selected points (A)–(E) lie in or around these pockets of large cross section, we can regard our results, obtained by neglecting the production of a $\tilde{\chi}_1^\pm \tilde{\chi}_2^\mp$ pair, to have uncertainties of this order. However, as we shall see later, this excess cross section will be distributed over a wealth of possible final states, so that the actual uncertainties in estimating many of these will be considerably reduced.

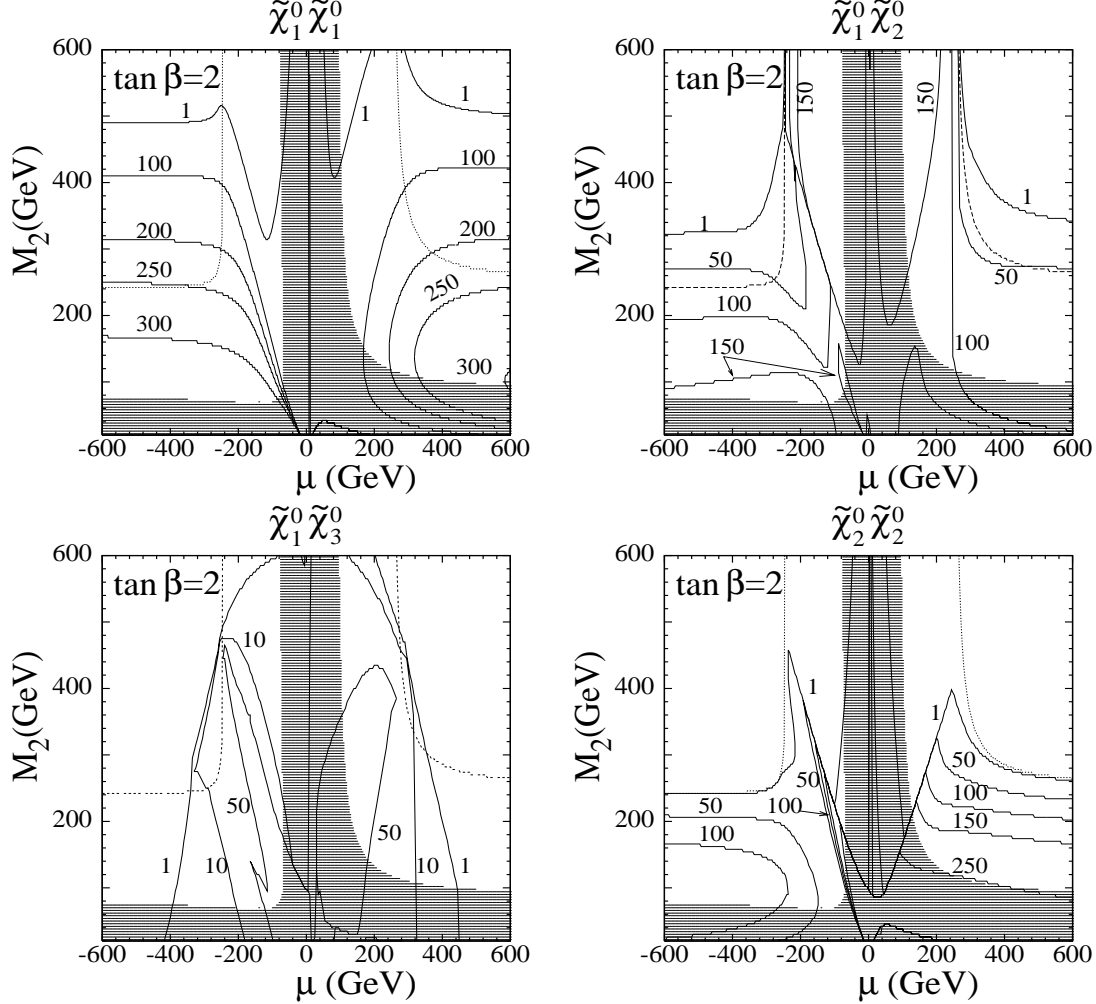


Figure 6. Contours of cross section (marked in fb) for production at the NLC of a pair of neutralinos for $\tan \beta = 2$ and $M_{\tilde{e}_L} = M_{\tilde{e}_R} = 150$ GeV.

In Fig. 6, we present contours of cross section (in fb) for the following pairs: (a) $\tilde{\chi}_1^0 \tilde{\chi}_1^0$, (b) $\tilde{\chi}_1^0 \tilde{\chi}_2^0$, (c) $\tilde{\chi}_1^0 \tilde{\chi}_3^0$, (d) $\tilde{\chi}_2^0 \tilde{\chi}_2^0$, all for $\tan \beta = 2$. For this plot the left and right selectrons are assumed to be degenerate, with the mass being fixed at 150 GeV. Fig. 7 represents an identical plot with $\tan \beta = 20$. A glance at the cross sections for production of $\tilde{\chi}_3^0$ in association with an LSP, $\tilde{\chi}_1^0$, shows that the production cross section is as severely suppressed (if not more), compared to the lighter neutralino states as is the case of the heavy chargino. Thus, we may feel justified in neglecting the $\tilde{\chi}_3^0$ as well as the heavier $\tilde{\chi}_4^0$ and $\tilde{\chi}_2^\pm$ states. As before, this would lead to an error of 15–20% at most, which would again be spread out over a multitude of decay modes.

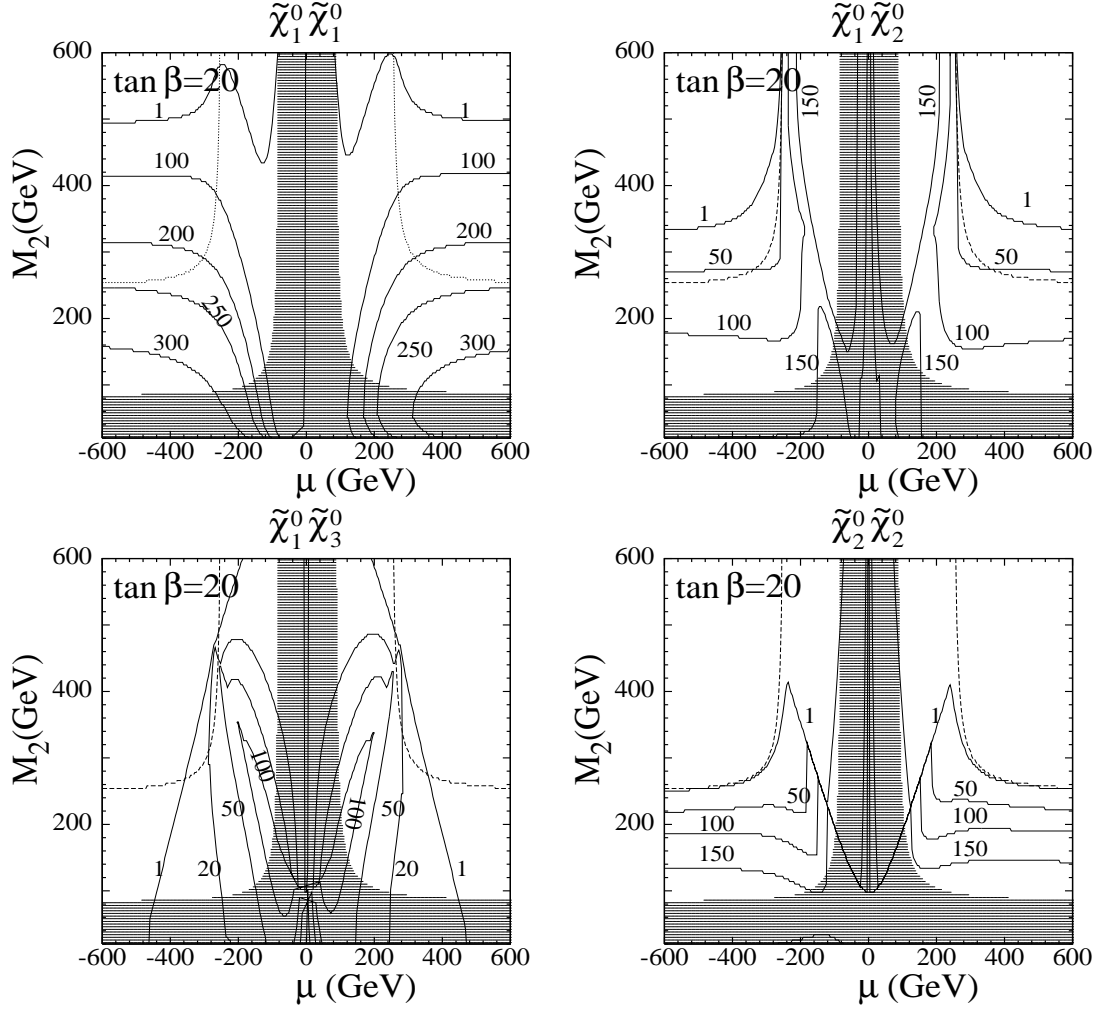


Figure 7. Same as Fig. 6, but with $\tan \beta = 20$.

Before concluding this section, some more general remarks are in order. In the first place, the variation of the cross section with the mass of the exchanged slepton as exhibited in Figs. 2 and 3 is more-or-less straightforward to explain, given the composition of the sparticles. The more complex variation of the cross section with the parameters which make up the chargino and neutralino mass matrices is shown in Figs. 5–7. These arise in a complicated way through the diagonalization procedure and one cannot develop easy physical arguments as to why the cross section is large or small. The dark shading in Figs. 5–7 represents the region ruled out by the chargino search at LEP-2 (running at 183 GeV) and corresponds to the contour of (lighter) chargino mass $m_{\tilde{\chi}_1^\pm} < 91$ GeV. Searches for both R -parity-conserving and R -parity-violating supersymmetry at the four LEP collaborations have essentially pushed the chargino mass to the kinematic limit[18], irrespective of the nature of the R -parity-violating operator. The broken line represents the contours of chargino mass $m_{\tilde{\chi}_1^\pm} = 250$ GeV, which represents the kinematic limit for chargino pair-production at the 500 GeV NLC. Of course, the sample points (A)–(E) chosen for our analysis lie outside the LEP-2 ruled-out region.

For Figs. 5–7, we have chosen the selectron masses to be $M_{\tilde{e}_L} = M_{\tilde{e}_R} = 150$ GeV. This is well above the range of LEP-2, but it should be possible to pair-produce selectrons of this mass at the 500 GeV NLC. Each of these selectrons can have the following decays[30]:

- to an electron and a neutralino;
- to a neutrino and a chargino (left selectron only);
- to a lepton and a neutrino (if there are L -violating operators of the $LL\bar{E}$ form), or a pair of quarks (if there are L -violating operators of the $LQ\bar{D}$ form).

Of these channels, in the weak R -parity-violation limit, we can neglect the third. For a right selectron, this means a unit branching ratio into electron and neutralino. For a pair of left selectrons, we can have in the final states:

$$e^+e^-\tilde{\chi}^0\tilde{\chi}^0, \quad e^+\nu\tilde{\chi}^0\tilde{\chi}^-, \quad e^-\bar{\nu}\tilde{\chi}^0\tilde{\chi}^+, \quad \nu\bar{\nu}\tilde{\chi}^+\tilde{\chi}^-,$$

where all possible neutralinos and charginos allowed by kinematics will contribute. The first channel usually has the largest branching ratio and will have essentially the same signals as those which form the subject of this article, together with an extra electron–positron pair with large energies and transverse momenta. For the other signals, the chargino will decay through its gauge couplings to $\tilde{\chi}_i^\pm \rightarrow \tilde{\chi}_j^0 f \bar{f}'$ where f and f' are fermions differing by one unit in charge. Thus we will have a pair of neutralinos in the final state, accompanied by various combinations of electrons, jets and neutrinos contributing to missing energy. Another possibility which, in general, needs to be considered[31], is that of production of a pair of sneutrinos $\tilde{\nu}_e$. If the left selectron has a mass of 150 GeV, the mass of the sneutrino $\tilde{\nu}_e$ will be close to this, the relation between the masses telling us that the sneutrino mass lies between 139–150 GeV, depending on the value of $\tan\beta$. These sneutrinos will certainly be pair-produced in e^+e^- interactions at 500 GeV. The decay modes will be analogous to those of the selectron, with similar final states. A comprehensive discussion of all these signals is desirable, but is beyond the scope of this work, which concentrates on pair-production and decay of charginos and neutralinos. However, we can guess that the signals and analysis will be very similar.

For selectron masses above 250 GeV, it will not be possible to produce selectron pairs at the 500 GeV NLC, and their effects will appear solely in chargino and neutralino pair-production. The sneutrino pair-production will be either suppressed or disallowed since the masses are close to or above the kinematic limit for somewhat larger selectron masses. In this case, the only possibility for detection of R -parity violation at the NLC will be through the signals discussed in this article, though, it must be admitted that larger selectron masses often lead to lower cross sections, as shown in Figs. 2 and 3. However, as the following discussions will show, a reduction in the cross sections by a factor as large as 2 could still yield substantial signals.

3. Chargino and Neutralino Decays

In this article, we assume that the lightest neutralino is the LSP. This is not forced upon us by cosmological arguments since we allow the LSP to decay, but, as explained in the Introduction, it is a convenient hypothesis to make. The other assumption we make is that of all the R -parity-violating couplings, only one is dominant. This is also an *ad hoc* assumption, but it mimics the case of the SM Yukawa couplings, where the top quark coupling is much larger than the others. In such a scenario, it is possible to isolate signals arising from the LSP decay, and this is what we analyze.

Once produced, the charginos and higher neutralinos will decay through various channels into final states containing the LSP, which will then decay into multi-fermion channels through R -parity-violating couplings. Since these are fairly well known[29, 32], we have not reproduced the formulae for each of these decay modes but include a general discussion of all the channels.

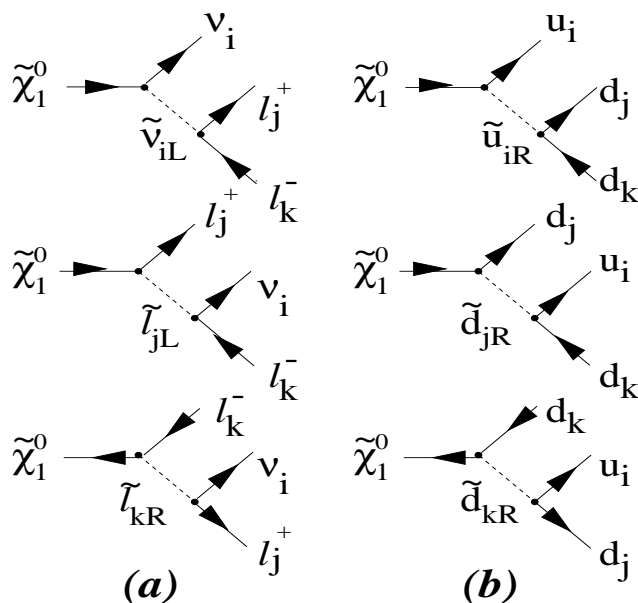


Figure 8. Feynman diagrams contributing to the decay of the LSP in the case of (a) L -violation with λ couplings, and (b) B -violation with λ'' couplings. The case of λ' couplings can be obtained by replacing $\nu_i \ell_j^+ \ell_k^- \rightarrow \nu_i d_j \bar{d}_k$ or $\ell_i^- u_j \bar{d}_k$ in (a).

The most important decay of all these is, of course, the decay of the LSP, which is the principal theme of this work. This can occur through the diagrams of Fig. 8(a) and (b), which are mediated by sfermions. If the R -parity-violating operator is of the $LL\bar{E}$ type, the final states will have two charged leptons and one neutrino, the flavours being determined by the single (dominant) coupling involved. If the R -parity-violating coupling is of the $LQ\bar{D}$ type, the final states will have two quarks and one charged lepton, or two quarks and one neutrino. The relevant diagrams for the neutrino case can be obtained from those in Fig. 8(a) by replacing each charged lepton ℓ with a d -type quark. The charged lepton case can then be obtained from this by replacing the neutrino by a charged lepton and the d -type quark by a u -type quark. The LSP decay will result in either two hadronic jets accompanied

by a charged lepton, or two jets and missing momentum. Finally, if the R -parity-violating coupling is of the $\bar{U}\bar{D}\bar{D}$ type, then the final state will generally consist of three hadronic jets. These modes are summarized below, where J denotes a hadronic jet.

$$\tilde{\chi}_1^0 \rightarrow \ell_1^+ \ell_2^- + \cancel{E}_T \quad (\text{for } LLE\bar{E}), \quad \tilde{\chi}_1^0 \rightarrow \ell^\pm JJ \text{ or } JJ + \cancel{E}_T \quad (\text{for } LQ\bar{D}), \quad \tilde{\chi}_1^0 \rightarrow 3J \quad (\text{for } \bar{U}\bar{D}\bar{D}),$$

Formulae arising from the evaluation of these diagrams are presented in Appendix A, where they agree with those already available in the literature [33]. Each of these cases is discussed separately in the following three sections, possible signals and backgrounds being identified and estimated. Since the LSP has only one decay mode, its branching ratio is always unity, and hence there is no dependence on the actual magnitude of the R -parity-violating coupling involved. This is an important point, since it enables us to make our analysis in the weak R -parity-violation limit, and renders our results robust in the sense that they are insensitive to the actual value of the R -parity-violating couplings involved. It is also worth drawing attention to the fact that, since we regard the lightest neutralino as the LSP, there is no possibility of sfermion resonances in its decay.

When we come to the higher neutralinos and charginos, the situation becomes rather complex, since all decays allowed by kinematic considerations can occur. It follows that what may actually be expected to occur depends strongly on the point in the MSSM parameter space. We must, therefore, consider, in the general case, all possible decays of each chargino and/or neutralino. The decay of the heavier chargino to the lighter chargino occurs essentially through the diagrams of Fig. 1(a), where the e^+e^- pair can be replaced by any pair of fermions. The decay of one neutralino to a different neutralino occurs through the diagrams of Fig. 1(b), where, once again, the e^+e^- pair is suitably replaced. It is also possible for a chargino to decay into a lighter neutralino or vice versa. Since all these decay channels have to be considered, it is convenient to make a little summary of the possibilities, and this is presented below. As before, we denote a hadronic jet by J . It must be borne in mind that the actual number of jets seen will not always be the same as in the list below, since jets can be missed if they are soft or if they merge into other jets. Similarly charged leptons will be observed only if they pass all the acceptance cuts.

$$\begin{aligned} \tilde{\chi}_2^0 &\rightarrow \tilde{\chi}_1^0 \ell^+ \ell^- && \text{or } \tilde{\chi}_1^0 + \cancel{E}_T && \text{or } \tilde{\chi}_1^0 JJ \\ &\leftrightarrow \tilde{\chi}_j^\pm \ell^\mp + \cancel{E}_T && \text{or } \tilde{\chi}_j^\pm JJ \quad (j = 1, 2) \\ \\ \tilde{\chi}_3^0 &\rightarrow \tilde{\chi}_i^0 \ell^+ \ell^- && \text{or } \tilde{\chi}_i^0 + \cancel{E}_T && \text{or } \tilde{\chi}_i^0 JJ \quad (i = 1, 2) \\ &\leftrightarrow \tilde{\chi}_j^\pm \ell^\mp + \cancel{E}_T && \text{or } \tilde{\chi}_j^\pm JJ \quad (j = 1, 2) \\ \\ \tilde{\chi}_4^0 &\rightarrow \tilde{\chi}_i^0 \ell^+ \ell^- && \text{or } \tilde{\chi}_i^0 + \cancel{E}_T && \text{or } \tilde{\chi}_i^0 JJ \quad (i = 1, 2, 3) \\ &\leftrightarrow \tilde{\chi}_j^\pm \ell^\mp + \cancel{E}_T && \text{or } \tilde{\chi}_j^\pm JJ \quad (j = 1, 2) \\ \\ \tilde{\chi}_1^\pm &\rightarrow \tilde{\chi}_i^0 \ell^\pm + \cancel{E}_T && \text{or } \tilde{\chi}_i^0 JJ \quad (i = 1, 2, 3, 4) \end{aligned}$$

$$\begin{aligned}
\tilde{\chi}_2^\pm &\rightarrow \tilde{\chi}_1^\pm \ell^+ \ell^- && \text{or } \tilde{\chi}_1^\pm + \cancel{E}_T && \text{or } \tilde{\chi}_1^\pm JJ \\
&\hookrightarrow \tilde{\chi}_i^0 \ell^\pm + \cancel{E}_T && \text{or } \tilde{\chi}_i^0 JJ && (i = 1, 2, 3, 4)
\end{aligned}$$

This complex set of options is illustrated in Fig. 9, where a typical mass spectrum is chosen and possible decays are represented as transitions from a higher state to a lower. The left side shows the most general case, when all possible cascade decays are considered. It is straightforward to count that there are 15 possible decays when only the charginos and neutralinos are considered, and, if we include the fact that either leptonic or hadronic final states can occur, one has a total of 35 channels to consider. When this is combined with the fact that a *pair* of charginos or neutralinos is produced in e^+e^- collisions, with all sorts of combinations for the decays of each being possible, it is obvious that a complete study is a gigantic task and well beyond the scope of our present analysis. Fortunately, it proves possible to carry out a meaningful analysis using only a subset of these production and decay channels. The chief reason for this is that the heavier neutralino and chargino states can be ignored in a first analysis, as we have explained in the previous section. Moreover, it is well known that, for a large part of the parameter space, the next-to-lightest neutralino $\tilde{\chi}_2^0$ is nearly degenerate with the lighter chargino $\tilde{\chi}_1^\pm$, so that its decay modes to the charginos (or vice versa) are suppressed, if not forbidden. This certainly happens for the five points where we have performed our analysis. A similar phenomenon occurs with the heavier chargino and the heaviest neutralino. The corresponding decay modes have very little available phase space and may be ignored without much loss of generality.

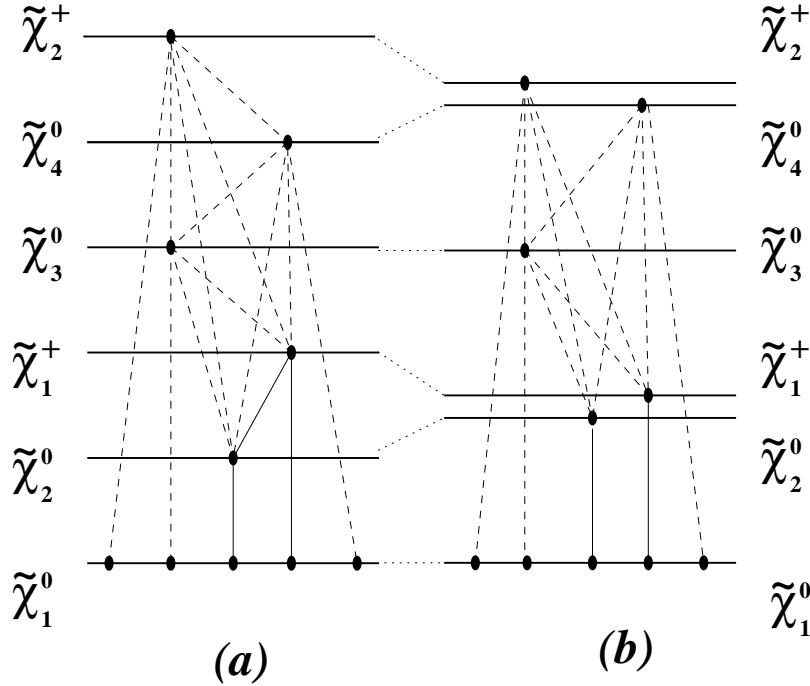


Figure 9. Schematic diagram showing all possible cascade decays of higher charginos and neutralinos to the LSP in (a) the most general case, and (b) a simplified case where two pairs of states are almost degenerate. Broken lines indicate possible decays; solid lines indicate those which have been considered in this article.

We now concentrate on the final states which could be of interest at a 500 GeV e^+e^- collider. As we have explained in detail in the previous section, these involve only the lowest three states in Fig. 9, and correspond, on the left of Fig. 9 to the three decays denoted by solid lines. If we take into account the approximate degeneracy of the $\tilde{\chi}_2^0$ and the $\tilde{\chi}_1^\pm$, this is reduced, on the right of Fig. 9, to just two decay modes. Of course, these two lines really denote five decay modes, since $\tilde{\chi}_2^0 \rightarrow \tilde{\chi}_1^0 + (\ell^+\ell^- \text{ or } \nu\bar{\nu} \text{ or } q\bar{q})$ and $\tilde{\chi}_1^\pm \rightarrow \tilde{\chi}_1^0 + (\ell^\pm\nu \text{ or } q\bar{q}')$. However, this number is manageable, even when all the combinatorics are taken into account, and we shall consider all these channels in the subsequent analysis.

Our analysis is also limited to the case when the t -quark (either on shell or off-shell) appear in the decays of the LSP, *i.e.* the couplings λ'_{i3k} and λ''_{3jk} do not form part of our analysis. Our studies were done using a parton-level Monte Carlo event generator, which does not yield high-quality results so far as hadronic jets are concerned, but which does enable us to get a quick and more-or-less correct picture of the signals that might be visible at the NLC.

4. Signals from $LL\bar{E}$ Operators

In this section, we concentrate on the signals that could be seen in the case when the R -parity is violated by $LL\bar{E}$ couplings. As explained in the previous section, the LSP will decay into a pair of charged leptons, with missing energy from a neutrino. Thus, if we consider the basic process, *i.e.*, a pair of LSP's being produced, then the final state will have *four* charged leptons and missing energy. The flavour of these leptons will be determined by the coupling responsible and cannot be predicted *á priori*, unless the coupling is known beforehand. If some of the heavier states are produced, then there will be additional leptons or jets in the final state from cascade decays. We make a list of these possibilities below and discuss each.

For the production of a pair of LSP's, the final state will be $\tilde{\chi}_1^0\tilde{\chi}_1^0 \rightarrow \ell_1^+\ell_2^-\ell_3^+\ell_4^- + \cancel{E}_T$, where, of the four charged leptons in the final state, two will be of one flavour, and the other two will be of one (possibly different) flavour. Since there are two neutrinos contributing to the missing energy, and each neutralino undergoes a three-body decay, it will not be possible to reconstruct the mass of the LSP from these final states. However, a final state with four hard charged leptons and missing energy is sufficiently spectacular to permit easy detection. There will be Standard Model backgrounds, of course. The chief of these comes from WWZ production (W -pair production with a radiated Z), where all the gauge bosons decay through leptonic channels. This background is unimportant at LEP-2, which has insufficient energy to produce all the gauge bosons on-shell, but could, in principle, become significant at the 500 GeV NLC. It turns out, however, as we shall see, that this background is rather small when compared with the R -parity-violating signals in the multi-lepton channel.

We now come to the issue of the production of higher neutralino and chargino states and their cascade decays to the LSP. We reiterate that this can lead to complicated signals, which are rendered more so by the fact that each higher chargino/neutralino state can decay into a lower state and a gauge boson W, Z . The latter can then decay either leptonically or hadronically. For one neutralino decaying

to another, or the heavier chargino decaying into the lighter, we must also distinguish between the cases of decay into a pair of charged leptons and into a pair of neutrinos. Even at a single point in parameter space, this makes for a somewhat messy analysis, although we limit the analysis to the low-lying states $\tilde{\chi}_1^0, \tilde{\chi}_2^0$ and $\tilde{\chi}_1^\pm$.

The signals which can be observed in the presence of $LL\bar{E}$ operators can be analyzed in the following way[34]. We consider the basic process

$$e^+e^- \longrightarrow \tilde{\chi}_1^0\tilde{\chi}_1^0 \longrightarrow \ell_1^+\ell_2^-\ell_3^+\ell_4^- + \cancel{E}_T \quad (4\ell + \cancel{E}_T) \quad (5)$$

where two of the final state leptons are positively charged and two are negatively charged. Assuming that the $\tilde{\chi}_2^0$ and the $\tilde{\chi}_1^\pm$ are nearly degenerate and thus their decay into one another may be neglected (see above), the only cascade decays one needs to consider are those in which a $\tilde{\chi}_2^0$ or a $\tilde{\chi}_1^\pm$ goes into a $\tilde{\chi}_1^0$ and a pair of fermions. These processes then lead to the following signals.

$$\begin{aligned}
e^+e^- \longrightarrow \tilde{\chi}_1^0 + \tilde{\chi}_2^0 &\rightarrow \tilde{\chi}_1^0 + \tilde{\chi}_1^0\nu\bar{\nu} &&\longrightarrow 4\ell + \cancel{E}_T \\
&\hookrightarrow \tilde{\chi}_1^0 + \tilde{\chi}_1^0\ell^+\ell^- &&\longrightarrow 6\ell + \cancel{E}_T \\
&\hookrightarrow \tilde{\chi}_1^0 + \tilde{\chi}_1^0JJ &&\longrightarrow 4\ell + \cancel{E}_T + 2 \text{ jets} \\
\\
e^+e^- \longrightarrow \tilde{\chi}_2^0 + \tilde{\chi}_2^0 &\rightarrow \tilde{\chi}_1^0\nu\bar{\nu} + \tilde{\chi}_1^0\nu\bar{\nu} &&\longrightarrow 4\ell + \cancel{E}_T \\
&\hookrightarrow \tilde{\chi}_1^0\ell^+\ell^- + \tilde{\chi}_1^0\nu\bar{\nu} &&\longrightarrow 6\ell + \cancel{E}_T \\
&\hookrightarrow \tilde{\chi}_1^0\ell^+\ell^- + \tilde{\chi}_1^0\ell^+\ell^- &&\longrightarrow 8\ell + \cancel{E}_T \\
&\hookrightarrow \tilde{\chi}_1^0\nu\bar{\nu} + \tilde{\chi}_1^0JJ &&\longrightarrow 4\ell + \cancel{E}_T + 2 \text{ jets} \\
&\hookrightarrow \tilde{\chi}_1^0\ell^+\ell^- + \tilde{\chi}_1^0JJ &&\longrightarrow 6\ell + \cancel{E}_T + 2 \text{ jets} \\
&\hookrightarrow \tilde{\chi}_1^0JJ + \tilde{\chi}_1^0JJ &&\longrightarrow 4\ell + \cancel{E}_T + 4 \text{ jets} \\
\\
e^+e^- \longrightarrow \tilde{\chi}_1^+ + \tilde{\chi}_1^- &\rightarrow \tilde{\chi}_1^0\ell^+\nu + \tilde{\chi}_1^0\ell^-\bar{\nu} &&\longrightarrow 6\ell + \cancel{E}_T \\
&\hookrightarrow \tilde{\chi}_1^0\ell^+\nu + \tilde{\chi}_1^0JJ &&\longrightarrow 5\ell + \cancel{E}_T + 2 \text{ jets} \\
&\hookrightarrow \tilde{\chi}_1^0JJ + \tilde{\chi}_1^0\ell^-\bar{\nu} &&\longrightarrow 5\ell + \cancel{E}_T + 2 \text{ jets} \\
&\hookrightarrow \tilde{\chi}_1^0JJ + \tilde{\chi}_1^0JJ &&\longrightarrow 4\ell + \cancel{E}_T + 4 \text{ jets}
\end{aligned}$$

This is not the end of the story, however, since every particle produced in the final state is not always visible, given the kinematic cuts and detector acceptances. We have chosen the following criteria for observability of leptons/jets at a 500 GeV e^+e^- machine:

$$p_T^\ell > 10 \text{ GeV} , \quad |\eta_\ell| < 3 , \quad p_T^J > 10 \text{ GeV} \quad \text{and} \quad |\eta_J| < 3 .$$

Moreover, we assume that two partons with an angular separation of $\delta R_{JJ} \equiv \sqrt{\delta\eta_{JJ}^2 + \delta\phi_{JJ}^2} < 0.7$ are merged into a single jet⁶. Similarly, a lepton will be assumed to be part of a jet if its angular separation $\delta R_{\ell J} < 0.4$. These cuts represent educated guesses and may change a little when realistic simulations

⁶We have checked that for our parton-level analysis the Durham and Jade algorithms for jet merging do not yield results substantially different from the cone algorithm used here.

become available. However, we do not expect the qualitative features of our analysis to change too much even if a better set of kinematic cuts becomes available.

Once all these criteria are applied, it is easy to see that signals with large numbers of final state leptons and/or jets are likely to get degraded to lower numbers of leptons and/or jets. Unobservable leptons and/or jets would make (small) contributions to the missing energy, augmenting the expectation from neutrinos produced in the final state. Counting signals by the number of leptons, we classify the observable final states as having 0–8 leptons with or without jets and always accompanied by substantial missing energy. To get an idea of the strength of the signal available from the above analysis, we show, in Table 3, the cross sections for these signals for different pair-production modes (in the case of a λ -coupling). We detail results for the five chosen points (A)–(E) in the parameter space. For each point, there are 13 different configurations: these correspond to the cases

- (a) $\tilde{\chi}_1^0 \tilde{\chi}_1^0$ pair production, where both LSP's decay to neutrino plus dilepton (1 configuration),
 - (b) $\tilde{\chi}_1^0 \tilde{\chi}_2^0$ pair production, where $\tilde{\chi}_2^0$ decays to $\tilde{\chi}_1^0 +$ neutrinos, dilepton or jets (3 configurations),
 - (c) $\tilde{\chi}_2^0 \tilde{\chi}_2^0$ pair production, where both $\tilde{\chi}_2^0$'s decay to $\tilde{\chi}_1^0 +$ neutrinos, dilepton or jets (6 configurations),
 - (d) $\tilde{\chi}_1^+ \tilde{\chi}_1^-$ pair production, where either chargino can decay to $\tilde{\chi}_1^0$ plus leptons or jets (3 configurations).
- After degradation, each of these makes a contribution to the signal with n leptons and missing energy (with or without jets). These contributions are summed and displayed in Table 3. It is interesting that though the basic process in this case starts with four leptons in the final state, a large fraction of these gets degraded into states with three (or even less) leptons. Fairly large cross sections may be obtained for final states with 4 to 6 leptons in the final state. When convoluted with a projected luminosity of about 10 fb^{-1} at the NLC, we see that these could yield some thousands of events every year. Though signals with 7 or 8 leptons are quite rare, given this large luminosity, we might expect to see a few of these too.

The last column of Table 3 gives the Standard Model background for each of these signals, where we have given the sum of the principal backgrounds (see Appendix C). It is immediately obvious that final states with one or two leptons have enormous backgrounds and cannot be used to look for R -parity violation. In any case, these arise, for the R -parity-violating signal, only as a result of degradation of signals with more leptons, and are not of primary interest. On the other hand, once the signal has three or more leptons the backgrounds are truly minuscule.

One other question which can arise is what we expect from the MSSM or other new physics[35] in case R -parity is conserved. In this case, instead of getting $4\ell + \cancel{E}_T$ from the pair of LSP's, we will simply get missing energy. A rough estimate of the signals can be made by simply mapping signals with n leptons in Table 3 to signals with $n - 4$ leptons. Keeping the backgrounds in mind, this means that it should still be possible to see signals with three and four leptons, but generally at a lower level than what would be the case if R -parity is violated. The absence of signals with more than four leptons would be a clear sign of R -parity-conserving supersymmetry. Alternatively, one could say that an unambiguous signal for R -parity-violating supersymmetry would be large numbers of events with 4, 5 and 6 leptons.

	Signal	$\tilde{\chi}_1^0 \tilde{\chi}_1^0$	$\tilde{\chi}_1^0 \tilde{\chi}_2^0$	$\tilde{\chi}_2^0 \tilde{\chi}_2^0$	$\tilde{\chi}_1^+ \tilde{\chi}_1^-$	Total Signal (fb)	Background (fb)
A	$1\ell + \cancel{E}_T$	1.1	0.4	0.2	1.5	3.2	8272.5
	$2\ell + \cancel{E}_T$	14.9	5.2	1.8	15.3	37.2	2347.4
	$3\ell + \cancel{E}_T$	91.7	25.3	7.2	71.6	195.8	1.5
	$4\ell + \cancel{E}_T$	212.8	49.6	13.6	152.8	428.8	0.4
	$5\ell + \cancel{E}_T$	0.0	37.8	19.3	113.5	170.6	–
	$6\ell + \cancel{E}_T$	0.0	39.6	21.6	26.9	88.0	–
	$7\ell + \cancel{E}_T$	0.0	0.0	11.9	0.0	11.9	–
	$8\ell + \cancel{E}_T$	0.0	0.0	8.0	0.0	8.0	–
B	$1\ell + \cancel{E}_T$	0.2	0.3	0.3	0.1	0.9	8272.5
	$2\ell + \cancel{E}_T$	4.5	6.1	5.6	2.0	18.1	2347.4
	$3\ell + \cancel{E}_T$	34.7	38.0	28.7	17.0	118.4	1.5
	$4\ell + \cancel{E}_T$	88.0	75.9	50.9	71.4	286.2	0.4
	$5\ell + \cancel{E}_T$	0.0	15.4	21.6	148.5	185.5	–
	$6\ell + \cancel{E}_T$	0.0	16.5	21.8	124.2	162.6	–
	$7\ell + \cancel{E}_T$	0.0	0.0	3.4	0.0	3.4	–
	$8\ell + \cancel{E}_T$	0.0	0.0	2.3	0.0	2.3	–
C	$1\ell + \cancel{E}_T$	0.3	0.2	0.6	0.5	1.6	8272.5
	$2\ell + \cancel{E}_T$	7.5	3.9	8.3	9.7	29.4	2347.4
	$3\ell + \cancel{E}_T$	56.3	23.1	39.1	61.9	180.4	1.5
	$4\ell + \cancel{E}_T$	140.0	44.9	66.3	151.3	402.5	0.4
	$5\ell + \cancel{E}_T$	0.0	11.6	36.2	93.6	141.4	–
	$6\ell + \cancel{E}_T$	0.0	13.1	37.6	16.9	67.6	–
	$7\ell + \cancel{E}_T$	0.0	0.0	7.3	0.0	7.3	–
	$8\ell + \cancel{E}_T$	0.0	0.0	5.3	0.0	5.3	–
D	$1\ell + \cancel{E}_T$	0.4	0.2	0.3	0.2	1.1	8272.5
	$2\ell + \cancel{E}_T$	7.8	3.8	5.0	4.6	21.2	2347.4
	$3\ell + \cancel{E}_T$	57.7	23.5	25.1	32.8	139.1	1.5
	$4\ell + \cancel{E}_T$	144.3	46.8	42.4	100.2	333.7	0.4
	$5\ell + \cancel{E}_T$	0.0	4.6	9.2	112.4	126.2	–
	$6\ell + \cancel{E}_T$	0.0	5.6	10.1	41.1	56.8	–
	$7\ell + \cancel{E}_T$	0.0	0.0	0.7	0.0	0.7	–
	$8\ell + \cancel{E}_T$	0.0	0.0	0.6	0.0	0.6	–
E	$1\ell + \cancel{E}_T$	0.2	0.1	0.1	0.0	0.4	8272.5
	$2\ell + \cancel{E}_T$	5.1	2.0	1.4	1.7	10.2	2347.4
	$3\ell + \cancel{E}_T$	45.9	16.0	11.6	17.6	91.1	1.5
	$4\ell + \cancel{E}_T$	136.7	42.8	28.5	66.1	274.1	0.4
	$5\ell + \cancel{E}_T$	0.0	3.1	4.4	77.4	84.9	–
	$6\ell + \cancel{E}_T$	0.0	4.8	6.3	27.9	38.9	–
	$7\ell + \cancel{E}_T$	0.0	0.0	0.3	0.0	0.3	–
	$8\ell + \cancel{E}_T$	0.0	0.0	0.3	0.0	0.3	–

Table 3. Showing the contribution (in fb) of different (light) chargino and neutralino production modes to multi-lepton signals at the NLC in the case of λ couplings. The last column shows the SM background.

In addition to this table, we present, in Fig. 10(a), the distribution in missing energy corresponding to the multi-lepton cases above for the point (A) in the parameter space. As expected, the missing energy grows progressively softer as more and more leptons are seen: this is partly because these correspond to states with less neutrinos and partly because there are fewer undetected leptons which might have contributed to the missing energy. It is clear that a cut of 20 GeV on the minimum missing energy would leave the signal(s) practically unaffected and this can be used for background reduction.

Similarly, in Fig. 10(b), we present histograms showing the distribution in the number of jets corresponding to each of the leptonic signals. Again, quite naturally, there are fewer jets as the number of observed leptons grows larger. The point (A) in the parameter space is chosen for these plots. Though our construction and treatment of jets is rather primitive, we do not expect the qualitative features of this figure to change when a more sophisticated analysis is performed.

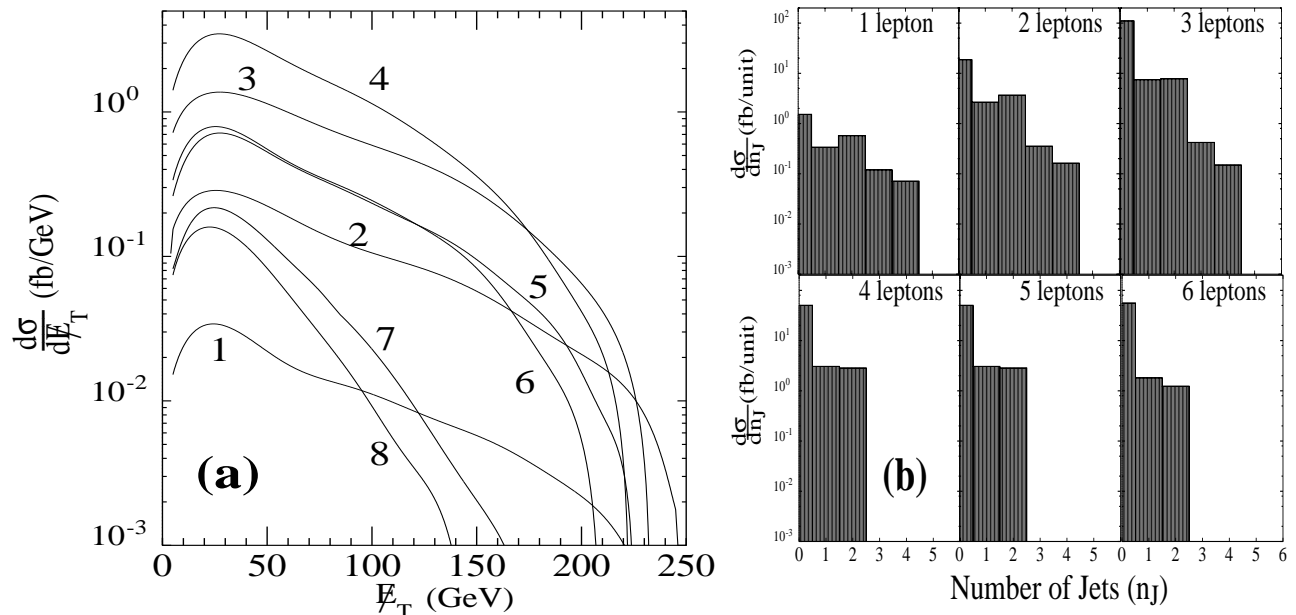


Figure 10. Illustrating the distribution in (a) missing transverse energy (E_T) and (b) the number of jets (n_J) when the LSP decays through a λ coupling. In (a) the number of observable leptons is marked next to the relevant curve.

In Table 3, which is essentially illustrative, we have not considered the particular λ_{ijk} coupling, but presented a common value for all flavour-combinations ijk . For better estimates, these must be appropriately convoluted with the respective detection efficiencies for e, μ and τ and also efficiency factors resulting from the different isolation criteria (from hadronic jets) for a τ jet as compared to an electron or a muon track[37]. This part of the analysis has not been done since ours is a preliminary study and we would like to obtain results of general interest. Though it renders our analysis somewhat crude, we would like to stress that the thrust of our work is in pinpointing the crucial role of the heavier chargino and neutralino states in detection of R -parity-violating signals at the NLC, for which, we feel, this level of analysis is adequate.

It is obvious that if R -parity is indeed violated through $LL\bar{E}$ operators and the LSP (alone or in association with one of the higher states) is produced and decays at the NLC, then it should be possible to see rather spectacular multi-lepton signals, even in one year of running. This itself would be a major cause of excitement, but a somewhat more tricky question would immediately arise: given that some signals are seen, can we identify the specific coupling responsible? In pursuit of this answer, we note that the lepton content of final states⁷ arising in LSP pair decay would be as follows:

$$\begin{aligned}
\lambda_{121} &: 4e, & 2e + 2\mu, & 3e + \mu; \\
\lambda_{122} &: 2e + 2\mu, & 4\mu, & e + 3\mu; \\
\lambda_{123} &: 2e + 2\tau, & 2\mu + 2\tau, & e + \mu + 2\tau; \\
\lambda_{131} &: 4e, & 2e + 2\tau, & 3e + \tau; \\
\lambda_{132} &: 2e + 2\mu, & 2\mu + 2\tau, & e + 2\mu + \tau; \\
\lambda_{133} &: 2e + 2\tau, & 4\tau, & e + 3\tau; \\
\lambda_{231} &: 2e + 2\mu, & 2e + 2\tau, & 2e + \mu + \tau; \\
\lambda_{232} &: 4\mu, & 2\mu + 2\tau, & 2\mu + \tau; \\
\lambda_{233} &: 2\mu + 2\tau, & 4\tau, & \mu + 3\tau.
\end{aligned}$$

Since all chargino and neutralino production modes are expected to end in a pair of LSP's, which will then decay to the above flavour combinations, one has to look at all multi-lepton states and identify the common components. Thus, an exhaustive tabulation of the final states should be able to tell us which flavour-combinations recur. From this we can infer the coupling responsible, with at most a twofold or threefold ambiguity. Though degradation of the number of leptons will tend to obscure the issue, there should be enough four (or more)-lepton final states produced directly through decay of the LSP to render some sort of identification possible. We might then look to other physics areas, perhaps precision measurement of lepton masses and other similar parameters, to clinch the identification, and perhaps extract the value of the coupling, which this analysis cannot give.

5. Signals with $LQ\bar{D}$ Operators

When we turn to the case of $LQ\bar{D}$ operators, the situation becomes more complex. In the first place, as explained above, the LSP has two decay modes, each with equal probability, but leading to rather different signatures. The decay to a charged lepton and two jets will lead, for $\tilde{\chi}_1^0\tilde{\chi}_1^0$ production, to a signal with an observable dilepton and (up to) four jets. The other mode will lead to (up to) four jets with substantial missing energy and momentum. One can also have a situation with one neutralino $\tilde{\chi}_1^0$ decaying into either channel, which leads to a single charged lepton, missing energy and (up to) four jets. This last signal will be enhanced by a combinatoric factor of 2. Each signature will have large backgrounds. However, in the first case, because of the Majorana nature of the neutralinos, it may be possible to see *like-sign* dileptons (LSD's), which have very little background from SM processes.

⁷ It is interesting that in the case of $LL\bar{E}$ couplings, the Majorana nature of the neutralinos (both the LSP and the higher ones) has no influence on the final states seen. This renders charge identification irrelevant.

When cascade decays of the heavier chargino and neutralino states are included in our analysis, the situation becomes even more complicated. If we merely consider their hadronic decays to the LSP, one could see the above signals, but with an increased hadronic component. However, the higher states can have leptonic decay modes too, and these will interfere with or augment the leptonic signals, as the case may be. Accordingly, one has to analyze the different signals with great care.

As in the previous section, we can analyze the signals in terms of the various pair-production modes and the cascade decays. The basic processes from pair-production of LSP's are

$$\begin{aligned}
e^+e^- &\longrightarrow \tilde{\chi}_1^0 + \tilde{\chi}_1^0 \longrightarrow \ell^\pm q\bar{q}' + \ell^\pm q\bar{q}' \longrightarrow 2\ell + 4 \text{ jets} \\
&\hookrightarrow \nu q\bar{q} + \ell^\pm q\bar{q}' \longrightarrow \ell + \cancel{E}_T + 4 \text{ jets} \\
&\hookrightarrow \nu q\bar{q} + \nu q\bar{q} \longrightarrow \cancel{E}_T + 4 \text{ jets}
\end{aligned}$$

The first channel (which comprises a quarter of the signal) consists of equal numbers of like-sign and unlike-sign dileptons. The signal with unlike-sign dileptons will have large SM backgrounds especially from ZZ , $t\bar{t}(g)$ and $\ell^+\ell^-Z$ channels (see Appendix C). The signal with like-sign dileptons will, on the other hand, have practically no backgrounds and constitute a ‘smoking gun’ signal for the presence of Majorana neutralinos in the decay chain. It is well to point out, however, that the only contributions to LSD signals will come only when both leptons come from the decay of LSP's. Leptonic decays of higher states to the LSP will never create LSD pairs, though they may augment the LSD signal arising from the decay of a $\tilde{\chi}_1^0\tilde{\chi}_1^0$ pair. We shall discuss this issue in more detail after enumerating the various decay modes and cross sections associated with the higher states.

The second channel (which comprises half of the signal) consists of a charged lepton, with missing energy and jets, where the lepton can be of either sign. As shown in Appendix C, this will have huge SM backgrounds, with contributions from several channels. Isolation of R -parity-violating signals from the background would require the careful application of kinematic cuts. For example, the $t\bar{t}$ background can be simply eliminated by requiring that no set of three jets should have an invariant mass in the neighborhood of the known top quark mass. The backgrounds with W 's and Z 's in the final state can be similarly handled if we require no pair of jets to reconstruct to the W and Z masses. However, it must be pointed out that with the usual uncertainties involved in jet reconstruction and the huge size of the backgrounds, isolation of the signal may not be possible over the *entire* parameter space. In fact, we may expect it to be possible only when the signal has fairly large values, *e.g.*, at point (A) in the parameter space (see Table 4).

The last channel, which requires one to trigger on missing energy, is not perhaps, the most rewarding mode to look for. In the first place, it comprises just one-fourth of the signal. Moreover, it may be mimicked by faulty reconstruction of jets, always a possibility when fragmentation is taken into account. In our analysis, therefore, we have not taken this channel into account, except in the case of higher state decays where it serves to augment the other multi-lepton signals.

For the higher states, we restrict ourselves, once again, to the $\tilde{\chi}_2^0$ and the $\tilde{\chi}_1^\pm$. Then, the processes

of interest are

$e^+e^- \longrightarrow \tilde{\chi}_1^0 + \tilde{\chi}_2^0$	$\rightarrow \tilde{\chi}_1^0 + \tilde{\chi}_1^0 \nu \bar{\nu}$	$\rightarrow 2\ell + \cancel{E}_T + 4 \text{ jets}$	or $\ell + \cancel{E}_T + 4 \text{ jets}$		
	$\hookrightarrow \tilde{\chi}_1^0 + \tilde{\chi}_1^0 \ell^+ \ell^-$	$\rightarrow 4\ell + 4 \text{ jets}$	or $3\ell + \cancel{E}_T + 4 \text{ jets}$	or $2\ell + \cancel{E}_T + 4 \text{ jets}$	
	$\hookrightarrow \tilde{\chi}_1^0 + \tilde{\chi}_1^0 JJ$	$\rightarrow 2\ell + 4 \text{ jets}$	or $\ell + \cancel{E}_T + 4 \text{ jets}$		
$e^+e^- \longrightarrow \tilde{\chi}_2^0 + \tilde{\chi}_2^0$	$\rightarrow \tilde{\chi}_1^0 \nu \bar{\nu} + \tilde{\chi}_1^0 \nu \bar{\nu}$	$\rightarrow 2\ell + \cancel{E}_T + 4 \text{ jets}$	or $\ell + \cancel{E}_T + 4 \text{ jets}$		
	$\hookrightarrow \tilde{\chi}_1^0 \ell^+ \ell^- + \tilde{\chi}_1^0 \nu \bar{\nu}$	$\rightarrow 4\ell + \cancel{E}_T + 4 \text{ jets}$	or $3\ell + \cancel{E}_T + 4 \text{ jets}$	or $2\ell + \cancel{E}_T + 4 \text{ jets}$	
	$\hookrightarrow \tilde{\chi}_1^0 \ell^+ \ell^- + \tilde{\chi}_1^0 \ell^+ \ell^-$	$\rightarrow 6\ell + 4 \text{ jets}$	or $5\ell + \cancel{E}_T + 4 \text{ jets}$	or $4\ell + \cancel{E}_T + 4 \text{ jets}$	
	$\hookrightarrow \tilde{\chi}_1^0 \nu \bar{\nu} + \tilde{\chi}_1^0 JJ$	$\rightarrow 2\ell + \cancel{E}_T + 6 \text{ jets}$	or $\ell + \cancel{E}_T + 6 \text{ jets}$		
	$\hookrightarrow \tilde{\chi}_1^0 \ell^+ \ell^- + \tilde{\chi}_1^0 JJ$	$\rightarrow 4\ell + 6 \text{ jets}$	or $3\ell + \cancel{E}_T + 6 \text{ jets}$	or $2\ell + \cancel{E}_T + 6 \text{ jets}$	
	$\hookrightarrow \tilde{\chi}_1^0 JJ + \tilde{\chi}_1^0 JJ$	$\rightarrow 2\ell + 8 \text{ jets}$	or $\ell + \cancel{E}_T + 8 \text{ jets}$		
$e^+e^- \longrightarrow \tilde{\chi}_1^+ + \tilde{\chi}_1^-$	$\rightarrow \tilde{\chi}_1^0 \ell^+ \nu + \tilde{\chi}_1^0 \ell^- \bar{\nu}$	$\rightarrow 4\ell + \cancel{E}_T + 4 \text{ jets}$	or $3\ell + \cancel{E}_T + 4 \text{ jets}$	or $2\ell + \cancel{E}_T + 4 \text{ jets}$	
	$\hookrightarrow \tilde{\chi}_1^0 \ell^+ \nu + \tilde{\chi}_1^0 JJ$	$\rightarrow 3\ell + \cancel{E}_T + 6 \text{ jets}$	or $2\ell + \cancel{E}_T + 6 \text{ jets}$	or $\ell + \cancel{E}_T + 6 \text{ jets}$	
	$\hookrightarrow \tilde{\chi}_1^0 JJ + \tilde{\chi}_1^0 \ell^- \bar{\nu}$	$\rightarrow 3\ell + \cancel{E}_T + 6 \text{ jets}$	or $2\ell + \cancel{E}_T + 6 \text{ jets}$	or $\ell + \cancel{E}_T + 6 \text{ jets}$	
	$\hookrightarrow \tilde{\chi}_1^0 JJ + \tilde{\chi}_1^0 JJ$	$\rightarrow 2\ell + 8 \text{ jets}$	or $\ell + \cancel{E}_T + 8 \text{ jets}$		

As in the case of $LL\bar{E}$ couplings, the actual number of leptons (and jets as well) will be degraded by kinematic cuts and detector acceptances. In Table 4 we set out the relative strengths of the various signals, with different numbers of leptons accompanied (always) by jets and (sometimes) by missing energy. One can again generate distributions analogous to those of Fig. 10, but these have not been presented here in the interests of brevity.

Just as we had 13 configurations in the case of $LL\bar{E}$ operators, in the present case we can have 68 configurations. These correspond to

- (a) $\tilde{\chi}_1^0 \tilde{\chi}_1^0$ pair production, with LSP's decaying to neutrino or lepton plus jets (4 configurations),
- (b) $\tilde{\chi}_1^0 \tilde{\chi}_2^0$ pair production, with the $\tilde{\chi}_2^0$ decaying to $\tilde{\chi}_1^0$ + neutrinos, dilepton or jets (12 configurations),
- (c) $\tilde{\chi}_2^0 \tilde{\chi}_2^0$ pair production, with either $\tilde{\chi}_2^0$ decaying to $\tilde{\chi}_1^0$ + neutrinos, dilepton or jets (36 configurations),
- (d) $\tilde{\chi}_1^+ \tilde{\chi}_1^-$ pair production, with either chargino decaying to $\tilde{\chi}_1^0$ + leptons or jets (16 configurations).

Each of these channels will make a contribution to the various multi-lepton signals. These are appropriately summed and displayed in Table 4.

Let us take a closer look at these various signals. The first channel, namely $\ell + \cancel{E}_T + \text{jets}$, has contributions from all the channels considered in Table 4 and this leads to a large cross section, but it also has a huge SM background and may not be the best option to look for $LQ\bar{D}$ couplings. The signal cross sections in Table 4 correspond typically to 2σ to 3σ fluctuations in the SM background. Mere observation of such an excess may not be enough to clinch the issue. However, it may still be worth looking for this channel after applying cuts to remove backgrounds where jets reconstruct to W and Z bosons, as discussed above. Unfortunately these cuts are also likely to remove much of the contributions from higher chargino and neutralino states, which actually contribute the bulk of the signal cross-section. It is not, therefore, clear that the mere observation of an excess in the $\ell + \cancel{E}_T + \text{jets}$ channel could be a signal for R -parity-violation in the $LQ\bar{D}$ form. However, an excess in this channel could be used to supplement signals seen in other channels, which are discussed below.

The second channel, which contains a dilepton, is the best option for this kind of search. As before

all chargino and neutralino production channels will contribute to this signal and the total cross section is reasonably high — certainly greater than the 4σ level for all the five points chosen for our analysis. This is the case irrespective of the charge of the leptons.

	Signal	$\tilde{\chi}_1^0\tilde{\chi}_1^0$	$\tilde{\chi}_1^0\tilde{\chi}_2^0$	$\tilde{\chi}_2^0\tilde{\chi}_2^0$	$\tilde{\chi}_1^+\tilde{\chi}_1^-$	Total Signal (fb)	Background (fb)
A	1 ℓ + jets	126.7	48.8	14.1	142.4	332.0	8262.5
	2 ℓ + jets	27.9	47.2	21.6	128.4	225.1	243.1
	3 ℓ + jets	0.0	28.0	21.8	48.4	98.2	1.5
	4 ℓ + jets	0.0	6.0	14.2	6.5	26.7	—
	5 ℓ + jets	0.0	0.0	6.3	0.0	6.3	—
	6 ℓ + jets	0.0	0.0	1.4	0.0	1.4	—
B	1 ℓ + jets	8.1	26.3	30.8	185.7	250.9	8262.5
	2 ℓ + jets	0.1	15.3	22.7	106.1	144.2	243.1
	3 ℓ + jets	0.0	1.1	5.0	8.3	14.4	1.5
	4 ℓ + jets	0.0	0.0	1.5	0.2	1.7	—
	5 ℓ + jets	0.0	0.0	0.1	0.0	0.1	—
	6 ℓ + jets	0.0	0.0	0.0	0.0	0.0	—
C	1 ℓ + jets	14.7	18.2	46.0	124.1	203.0	8262.5
	2 ℓ + jets	0.3	13.6	44.2	26.8	84.9	243.1
	3 ℓ + jets	0.0	1.2	11.7	2.0	14.9	1.5
	4 ℓ + jets	0.0	0.0	4.5	0.0	4.5	—
	5 ℓ + jets	0.0	0.0	0.4	0.0	0.4	—
	6 ℓ + jets	0.0	0.0	0.0	0.0	0.0	—
D	1 ℓ + jets	70.1	28.0	29.6	117.0	244.7	8262.5
	2 ℓ + jets	9.4	9.0	14.2	86.1	118.7	243.1
	3 ℓ + jets	0.0	2.6	5.5	27.2	35.3	1.5
	4 ℓ + jets	0.0	0.3	1.3	3.1	4.7	—
	5 ℓ + jets	0.0	0.0	0.2	0.0	0.2	—
	6 ℓ + jets	0.0	0.0	3.3	0.0	3.3	—
E	1 ℓ + jets	66.2	23.4	17.0	70.2	176.8	8262.5
	2 ℓ + jets	9.8	7.6	8.0	43.6	69.0	243.1
	3 ℓ + jets	0.0	2.2	2.6	26.8	31.6	1.5
	4 ℓ + jets	0.0	0.3	0.8	12.5	13.6	—
	5 ℓ + jets	0.0	0.0	0.2	0.0	0.2	—
	6 ℓ + jets	0.0	0.0	0.0	0.0	0.0	—

Table 4. Showing the contribution (in fb) of different (light) chargino and neutralino production modes to multi-lepton signals at the NLC in the case of λ' couplings. The last column shows the SM background.

We now come to the important issue of LSD signals. We have already explained that one-eighth of the $\tilde{\chi}_1^0\tilde{\chi}_1^0$ signal will consist of LSD's: this means 35, 0.1, 0.4, 12, 12 LSD events at the points (A)–(E) respectively, assuming an integrated luminosity of 10 fb^{-1} per year. These numbers assume 100% efficiency in charge identification, whereas a figure of around 70-80% would probably be more realistic. The strong variation in these numbers over the parameter space seems to indicate that one cannot confidently predict LSD signals everywhere. However, the actual situation is not so bad, because there will still be contributions from the cascade decays.

We can actually make a rough estimate of the contribution to LSD signals from cascade decays using Table 4 and assuming that the decay widths of the $\tilde{\chi}_2^0$ and $\tilde{\chi}_1^\pm$ are dominated by the Z and W -exchange channel respectively. This happens for a reasonably large part of the parameter space. In this case, we estimate that the actual numbers of LSD events with 10 fb^{-1} luminosity[23] will be around 180, 10, 75, 83 and 53 respectively for the points (A)–(E). If we recall that there is practically no SM background then, even with a charge detection efficiency of around 70%, we should see quite healthy numbers of like-sign dileptons in a year’s running of the NLC.

Signals with three or more leptons will, in general, have small SM backgrounds and should be seen without difficulty if the higher charginos and neutralinos have a significant branching ratio to leptons. This is certainly true of the points (A)–(E), but there do exist points in the parameter space where the higher states decay principally to the LSP accompanied by hadronic jets. In such cases, the multi-lepton signals will be suppressed, but we should get a larger *fraction* of LSD events. There is, thus, a trade-off, when we look at all the signals.

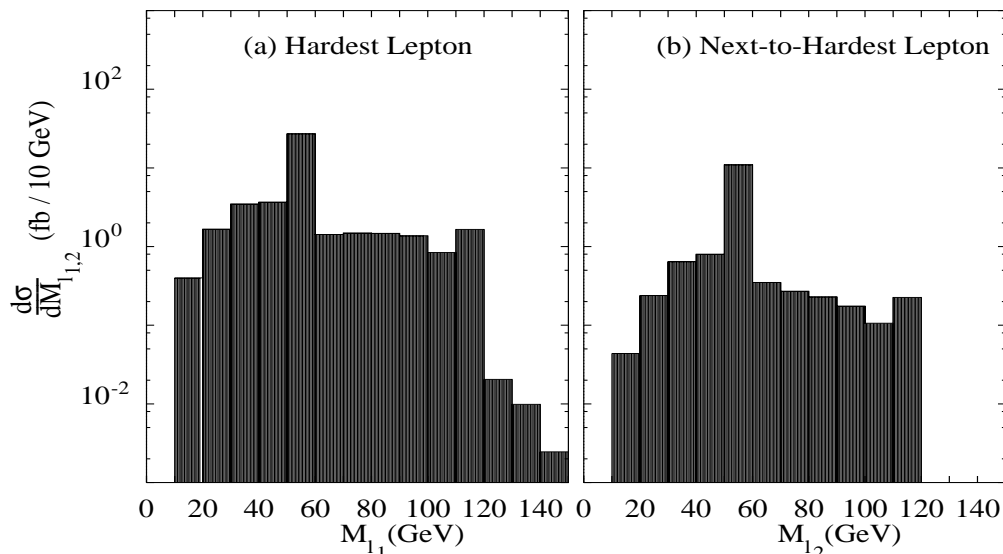


Figure 11. Illustrating the distribution in invariant mass reconstructed from (a) the hardest lepton and all jets in the same hemisphere, and (b) the next-to-hardest lepton and all hadronic jets in its hemisphere, when all contributions are summed over (signal only). The point (A) in the parameter space is chosen.

To conclude this section, we make a few remarks on the possibility of reconstructing the mass of the chargino and the neutralinos. A simple strategy is to focus on the n -lepton-plus-jets signal, with or without missing energy. Assuming that the (highly relativistic) neutralinos are produced back-to-back in the laboratory frame, we construct the invariant mass of the hardest lepton with all jets in the same hemisphere, where the direction of the hardest jet is taken to be the hemisphere axis. The invariant mass thus obtained should show a distinct peak at the LSP mass. Cascade decays will, however, tend to broaden the distribution. In Fig. 11 we have shown the invariant mass distribution from this construction using the point (A) in the parameter space. This is done for (a) the hardest lepton and

(b) the next-to-hardest lepton (with all jets in its hemisphere). It is interesting to note that both the distributions show a classic resonance at the LSP mass (in the bin 50–60 GeV) as well as a secondary peak at the mass of the next-to-lightest neutralino, or lightest chargino, both of which have masses in the same bin 110–120 GeV. The secondary peak is easily identified as the bin beyond which the distribution exhibits a sharp fall. If such a distribution is indeed seen above the background, we would be able to determine simultaneously *three* sparticle masses, those of the $\tilde{\chi}_1^0, \tilde{\chi}_2^0, \tilde{\chi}_1^\pm$ respectively. Such information can then be used to determine two⁸ of the three free parameters M_2, μ and $\tan\beta$. The measured cross-sections could then be used to yield information on the remaining parameter as well as the selectron masses. Much of this would depend, however, on whether the distributions seen in Fig. 11 can be seen above the background. We do not expect any of the background processes to show a strong resonant peak in this construction, but there would be a large continuum. A detailed analysis, using a proper jet reconstruction algorithm, needs to be performed, before this issue can be properly resolved. We leave this issue to be settled in a more focussed analysis in the future.

6. Signals with $\bar{U}\bar{D}\bar{D}$ Operators

The last case of R -parity-violation is that of $\bar{U}\bar{D}\bar{D}$ operators with λ'' couplings which arise in case baryon number is violated. As discussed in section 3, in this case, the LSP will simply decay into three hadronic jets. Thus the basic process with production of $\tilde{\chi}_1^0\tilde{\chi}_1^0$ will lead to a six-jet final state (with some jets lost through merging). In itself, this is not impossible to study, but there are two complications. The first is the usual case of higher state production and decay, which can lead to leptons in the final state, as well as (unwelcome) extra hadronic jets. The other is the large SM background from $t\bar{t}$ production, which can lead to six-jet final states if both the top quarks decay hadronically. Other backgrounds, such as those from WWZ production are not inconsiderable either. Thus, kinematic strategies are of paramount importance in this case, unlike the two previous cases, where a profusion of leptons in the final state makes detection easy.

The basic process in this case is

$$e^+e^- \longrightarrow \tilde{\chi}_1^0 + \tilde{\chi}_1^0 \longrightarrow udd (\bar{u}\bar{d}\bar{d}) + udd (\bar{u}\bar{d}\bar{d}) \longrightarrow 6 \text{ jets} \quad (6)$$

where sets of three jets have invariant masses peaking at the neutralino mass (assuming all the jets are seen) and the Majorana nature of $\tilde{\chi}_1^0$ is taken into account. With the introduction of cascades, we now have a large number of possibilities, as in the previous two cases. These are listed below.

$$\begin{aligned} e^+e^- \longrightarrow \tilde{\chi}_1^0 + \tilde{\chi}_2^0 &\rightarrow \tilde{\chi}_1^0 + \tilde{\chi}_1^0\nu\bar{\nu} &\rightarrow 6 \text{ jets} + \cancel{E}_T \\ &\leftrightarrow \tilde{\chi}_1^0 + \tilde{\chi}_1^0\ell^+\ell^- &\rightarrow 2\ell + 6 \text{ jets} \\ &\leftrightarrow \tilde{\chi}_1^0 + \tilde{\chi}_1^0JJ &\rightarrow 8 \text{ jets} \end{aligned}$$

⁸To determine all three, we would also require to know the (small) mass-splitting between the $\tilde{\chi}_2^0$ and the $\tilde{\chi}_1^\pm$. This would require a far better mass resolution than what we have assumed in this work.

$$\begin{aligned}
e^+e^- &\longrightarrow \tilde{\chi}_2^0 + \tilde{\chi}_2^0 &\rightarrow \tilde{\chi}_1^0\nu\bar{\nu} + \tilde{\chi}_1^0\nu\bar{\nu} &\rightarrow 6 \text{ jets} + \cancel{E}_T \\
&&\hookrightarrow \tilde{\chi}_1^0\ell^+\ell^- + \tilde{\chi}_1^0\nu\bar{\nu} &\rightarrow 2\ell + 6 \text{ jets} + \cancel{E}_T \\
&&\hookrightarrow \tilde{\chi}_1^0\ell^+\ell^- + \tilde{\chi}_1^0\ell^+\ell^- &\rightarrow 4\ell + 6 \text{ jets} \\
&&\hookrightarrow \tilde{\chi}_1^0\nu\bar{\nu} + \tilde{\chi}_1^0JJ &\rightarrow \cancel{E}_T + 8 \text{ jets} \\
&&\hookrightarrow \tilde{\chi}_1^0\ell^+\ell^- + \tilde{\chi}_1^0JJ &\rightarrow 2\ell + \cancel{E}_T + 6 \text{ jets} \\
&&\hookrightarrow \tilde{\chi}_1^0JJ + \tilde{\chi}_1^0JJ &\rightarrow 10 \text{ jets} \\
\\
e^+e^- &\longrightarrow \tilde{\chi}_1^+ + \tilde{\chi}_1^- &\rightarrow \tilde{\chi}_1^0\ell^+\nu + \tilde{\chi}_1^0\ell^-\bar{\nu} &\rightarrow 2\ell + \cancel{E}_T + 6 \text{ jets} \\
&&\hookrightarrow \tilde{\chi}_1^0\ell^+\nu + \tilde{\chi}_1^0JJ &\rightarrow \ell + \cancel{E}_T + 6 \text{ jets} \\
&&\hookrightarrow \tilde{\chi}_1^0JJ + \tilde{\chi}_1^0\ell^-\bar{\nu} &\rightarrow \ell + \cancel{E}_T + 6 \text{ jets} \\
&&\hookrightarrow \tilde{\chi}_1^0JJ + \tilde{\chi}_1^0JJ &\rightarrow 10 \text{ jets}
\end{aligned}$$

Of course, final states with such large numbers of jets will inevitably involve a great deal of jet merging, leading to states with (much) lower jet multiplicity. A similar study involving neutralino and chargino pair-production at LEP-1.5 has shown [38] that these lead dominantly to three- and four-jet final states. Thus, the jet multiplicities shown above should not be taken at all seriously.

The final states arising from cascades could contain one, two or even four leptons, as the case may be, and it might be possible to trigger on these in a search. The states with one or two leptons, as we have explained before, have large SM backgrounds, though, as the table shows, it might not be hopeless to look for an excess over the fluctuation in the background. The three and four-lepton signals will be easier to identify, but one must remember that they will come accompanied by (up to) six jets. We, therefore, require these leptons to satisfy isolation criteria to ensure that they are not, indeed, part of the jets themselves. Following the earlier sections, we present, in Table 5, a list of these multi-lepton signals, always accompanied by multiple jets and (sometimes) by missing energy.

In constructing this table, we consider a total of 17 configurations. These arise, like the previous ones from

- (a) $\tilde{\chi}_1^0\tilde{\chi}_1^0$ pair production, where each LSP decays to jets (1 configuration),
- (b) $\tilde{\chi}_1^0\tilde{\chi}_2^0$ pair production, with $\tilde{\chi}_2^0$ decaying to $\tilde{\chi}_1^0 +$ neutrinos, dilepton or jets (3 configurations),
- (c) $\tilde{\chi}_2^0\tilde{\chi}_2^0$ pair production, with either $\tilde{\chi}_2^0$ decaying to $\tilde{\chi}_1^0 +$ neutrinos, dilepton or jets (9 configurations),
- (d) $\tilde{\chi}_1^+\tilde{\chi}_1^-$ pair production, with either chargino decaying to $\tilde{\chi}_1^0 +$ leptons or jets (4 configurations).

As before, all these are summed and displayed in Table 5. Each signal may or may not be accompanied by missing energy.

Of course, if the jet multiplicity is not taken into account, then these signals will be rather similar to the (R -parity-conserving) MSSM backgrounds. This is because the leptons come entirely from the decays of the chargino and higher neutralino states to the LSP, irrespective of the decays of the LSP itself. Thus, in order to isolate signals for λ'' couplings, it is crucial to study the multi-jet content of the final state.

	Signal	$\tilde{\chi}_1^0\tilde{\chi}_1^0$	$\tilde{\chi}_1^0\tilde{\chi}_2^0$	$\tilde{\chi}_2^0\tilde{\chi}_2^0$	$\tilde{\chi}_1^+\tilde{\chi}_1^-$	Total Signal (fb)	Background (fb)
A	1 ℓ + jets	0.0	47.0	22.9	155.3	225.2	8262.5
	2 ℓ + jets	0.0	38.1	26.2	30.7	95.0	243.1
	3 ℓ + jets	0.0	0.0	12.5	0.0	12.5	1.5
	4 ℓ + jets	0.0	0.0	5.1	0.0	5.1	–
B	1 ℓ + jets	0.0	21.3	29.4	196.8	247.5	8262.5
	2 ℓ + jets	0.0	12.3	19.5	92.3	124.1	243.1
	3 ℓ + jets	0.0	0.0	3.2	0.0	3.2	1.5
	4 ℓ + jets	0.0	0.0	0.9	0.0	0.9	–
C	1 ℓ + jets	0.0	14.8	44.3	115.0	174.1	8262.5
	2 ℓ + jets	0.0	11.7	39.9	16.4	68.0	243.1
	3 ℓ + jets	0.0	0.0	7.7	0.0	7.7	1.5
	4 ℓ + jets	0.0	0.0	3.0	0.0	3.0	–
D	1 ℓ + jets	0.0	5.5	10.6	138.7	154.8	8262.5
	2 ℓ + jets	0.0	5.6	11.1	45.0	61.7	243.1
	3 ℓ + jets	0.0	0.0	0.8	0.0	0.8	1.5
	4 ℓ + jets	0.0	0.0	0.4	0.0	0.4	–
E	1 ℓ + jets	0.0	3.5	4.8	90.2	98.4	8262.5
	2 ℓ + jets	0.0	4.9	6.6	29.1	40.7	243.1
	3 ℓ + jets	0.0	0.0	0.4	0.0	0.4	1.5
	4 ℓ + jets	0.0	0.0	0.3	0.0	0.3	–

Table 5. Showing the contribution (in fb) of different (light) chargino and neutralino production modes to multi-lepton signals at the NLC in the case of λ'' couplings.

The question now arises: if we do indeed observe multi-jet signals, with or without leptons and/or missing energy, what strategy should we adopt in order to identify whether these arise from baryon-number-violating couplings, or from some other source? It is difficult to find a simple and all-encompassing answer. Perhaps the most straightforward solution is to appeal to kinematics and carry out mass reconstructions. Recognizing that the final state must always contain a pair of (generally) highly relativistic LSP's decaying into three jets apiece, we use the following strategy: the hardest jet in the final state is identified and its invariant mass is constructed with all the other jets lying in the same hemisphere. Then, we look for the hardest jet in the opposite hemisphere and again construct its invariant mass with all other jets lying in that hemisphere. We require these two invariant masses to lie within 10 GeV of each other, noting that if they are equal, or nearly equal, this is indicative of similar parentage. Once this criterion is satisfied, we plot the two invariant mass distributions to see if they show significant peaking. A similar strategy was followed by the ALEPH Collaboration in their study of the (now-defunct) four-jet anomaly [36]. In an earlier study[38] at LEP-1.5, it was shown that a modest peak does indeed form. In the present case, at the NLC, our results are illustrated in Fig. 12, for (a) the hardest jet and (b) the hardest jet in the opposite hemisphere. Once again, we have chosen the point (A) in the parameter space. It is clear from the figure that we have a clear resonance at the mass of the lightest neutralino, with a sharp cutoff at the mass of the second neutralino or

(light chargino). However, this cutoff may not be clearly observable because of the SM backgrounds, especially the one from $t\bar{t}$, which, though it will peak around m_t , will have a non-vanishing tail in the neighbourhood of 100–120 GeV. Backgrounds from W and Z bosons in the final state can be removed by requiring no two jets to have invariant masses in the vicinity of M_W and M_Z , though this cut has not actually been applied in Fig. 12. Application of the cut would probably reduce the cross-section somewhat, but make the resonance more sharp, since much of the smearing is due to hadronic decays of the chargino and higher neutralino states, which take place largely through W and Z exchanges.

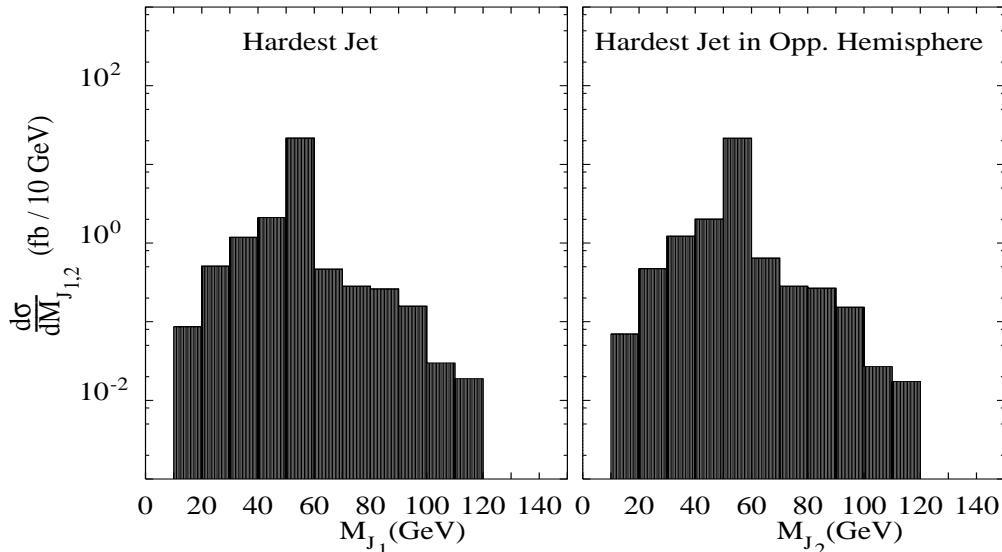


Figure 12. Illustrating the distribution in invariant mass reconstructed from (a) the hardest jet and all jets in the same hemisphere, and (b) the hardest jet in the opposite hemisphere and all remaining hadronic jets, when all contributions are summed over (signal only). The point (A) in the parameter space is chosen.

In case invariant mass distributions such as those shown in Fig. 12 are seen, it may be possible to determine the mass of the LSP, and the (degenerate) $\tilde{\chi}_2^0$ and $\tilde{\chi}_1^\pm$. As explained in the previous section, it might then be possible to determine some of the parameters of the MSSM; conversely, absence of the signals predicted here would constrain the parameter space (assuming the presence of λ'' couplings).

Finally, we remark on the possibility of identifying the λ'' coupling responsible for the signal seen. This must depend on flavour-tagging, which is far more difficult for hadrons than for leptons, and must be considered well-nigh impossible for the lighter quark flavours. b and c quarks may be tagged with some reasonable efficiencies, but, given the large number of jets and their large merging probabilities, we think it highly unlikely that any flavour-tagging worth the name can be achieved. It may be necessary to look to other physics possibilities to determine the exact nature of the coupling, assuming signals for a λ'' coupling are seen.

7. Summary and Conclusions

It might be well to go over the main points of our analysis again before ending. We have discussed chargino and neutralino pair production at a 500 GeV e^+e^- collider in the weak R -parity-violation limit, where the production modes are solely through the R -parity-conserving couplings and the lightest supersymmetric particle (LSP) decays purely through R -parity-violating couplings. Our analysis shows that it is sufficient to consider production of the two lightest neutralinos and of the lightest chargino. This simplifies matters considerably, since the higher chargino and neutralino states can have very complicated cascade decays, which would render the book-keeping almost an impossible task. We have indicated how a non-observation of supersymmetry signals at a 500 GeV machine would help us to make a very similar analysis at a 1 TeV machine.

We have then discussed the decays of the lightest neutralino (LSP) through the three types of R -parity-violating couplings assuming the top quark plays no role in these decays. At the same time we have considered decays of the (relevant) higher states to the LSP, with accompanying fermions. These result in a wealth of final state topologies, which we have classified by the number of hard isolated leptons. The observability of these leptons has been analyzed using a simple parton-level Monte Carlo event generator, which also enables us to get approximate distributions in missing energy and the jet-multiplicity in the final state. For λ -type couplings, the signal is basically an excess of multi-lepton states, together with substantial missing energy. For λ' -type couplings, the signal consists of leptons and multiple jets in the final state, but we utilize a rather simple-minded algorithm to reconstruct the LSP and higher neutralino masses (within some resolution). This actually works pretty well and enables us to predict that such signals, if seen, can be quite clearly identified as due to \mathcal{R}_p supersymmetry. We also show that if charge identification of final-state leptons can be carried out with reasonable efficiency, then like-sign dilepton (LSD) signals could be a very promising signal, insofar as they have practically no SM backgrounds. For λ'' couplings, a similar mass reconstruction is suggested: this shows a distinct resonance and could be again used to indicate \mathcal{R}_p supersymmetry. We have also discussed backgrounds and some simple strategies for their elimination, though a detailed simulation has not been attempted.

To conclude, then, we have made a detailed study of various possibilities for seeing the R -parity-violating version of the minimal supersymmetric Standard Model at a 500 GeV linear e^+e^- collider. It is hardly necessary to point out that one could make a very similar analysis at a muon collider of the same energy and luminosity unless this is tuned to a Higgs resonance. Given the lack of any concrete evidence of supersymmetry till date, and the fact that the R -parity-violating sector has very few theoretical constraints, the number of possible scenarios for such signals is extremely large. A complete treatment would be a massive task and probably not worth the effort at this early stage, when a 500 GeV e^+e^- machine exists only on paper. Nevertheless, we have isolated some of the important features of the problem, and have identified some useful approximations that bring a semblance of order to the multitude of cascade decays of higher chargino and neutralino states, which can be produced with quite reasonable cross sections at this energy. We hope that our work will encourage further studies of these extremely interesting signals.

Acknowledgments.

The authors are grateful to F. Boudjema, J. Kalinowski and B. Mukhopadhyaya for discussions. DKG would like to thank the Centre for Theoretical Studies, Indian Institute of Science, Bangalore, where a large part of this work was done, for hospitality. RMG acknowledges partial financial support from the Department of Science and Technology (India), the National Science Foundation, under NSF-grant-Int-9602567 and the Indo-French Collaboration no. 1701-1 *Collider Physics*. SR acknowledges the hospitality of the Laboratoire de Physique Particules (LAPP), Annecy, where a part of this work was done.

References

- [1] For reviews, see, for example, H. Nilles, *Phys. Rept.* **110**, 1 (1984) ; H. Haber and G. Kane, *Phys. Rept.* **117**, 75 (1985) ; J.F. Gunion, *Selected Low-Energy Supersymmetry Phenomenology Topics*, Presented at 29th International Conference on High-Energy Physics (ICHEP 98), Vancouver, Canada, 23-29 Jul 1998, hep-ph/9810394.
- [2] See, for example, M. Carena *et al.*, Argonne preprint ANL-HEP-PR-97-98 (1997), hep-ex/9712022, and references therein; also J.F. Grivaz, *Supersymmetric Particle Searches at LEP in Perspectives on Supersymmetry*, ed. G.L. Kane (World Scientific), p.179-203, hep-ph/9709505.
- [3] P. Fayet, *Phys. Lett.* **B69**, 489 (1977) ; G. Farrar and P. Fayet, *Phys. Lett.* **B76**, 575 (1978) .
- [4] For a recent review, see N. Fornengo, Univ. of Turin preprint DFTT-18-98 (1998), astro-ph/9804295.
- [5] S. Weinberg, *Phys. Rev.* **D26**, 287 (1982) ; N. Sakai and T. Yanagida, *Nucl. Phys.* **B197**, 533 (1982) ; C. Aulakh and R. Mohapatra, *Phys. Lett.* **B119**, 136 (1983) .
- [6] Y. Totsuka, in Proc. of the XXIV Conf. on High Energy Physics, Munich, 1988, Eds. R. Kotthaus and J.H. Kühn, (Springer-Verlag, 1989); Icarus Detector Group at the Int. Symposium on Neutrino Astrophysics, Takayama, 1992.
- [7] J.L. Goity and M. Sher, *Phys. Lett.* **B**, 346 (196) 9,95.
- [8] A.Yu. Smirnov and F. Vissani, *Phys. Lett.* **B380**, 317 (1996) and *Nucl. Phys.* **B460**, 37 (1996) .
- [9] L.E. Ibañez and G.G. Ross, *Phys. Lett.* **B260**, 291 (1991) and *Nucl. Phys.* **B368**, 3 (1992) .
- [10] H. Dreiner, *An Introduction to Explicit R-Parity Violation in Perspectives on Supersymmetry*, p.462-479, ed. G.L. Kane (World Scientific), hep-ph/9707435.
- [11] R. Barbier *et al*, *Report of the Group on the R-parity Violation*, hep-ph/9810232 (unpublished);
- [12] G. Bhattacharyya, *Nucl. Phys. Proc. Suppl.* **52 A**, 83 (1997) and references therein.
- [13] A.S. Joshipura and M. Nowakowski, *Phys. Rev.* **D51**, 2421 (1995) ; M. Nowakowski, in *Barcelona 1997, Quantum effects in the minimal supersymmetric standard model*, p.351-360.
- [14] L.J. Hall and M. Suzuki, *Nucl. Phys.* **B231**, 419 (1984) ; For a recent pedagogic review, see J.C. Romao, Univ. of Lisbon preprint FISIST-15-98-CFIF (1998), hep-ph/9811454.
- [15] D.P. Roy, *Phys. Lett.* **B283**, 27092; M. Guchait and D.P. Roy (19 *Phys. Rev.* **D**) **54**, 3276 (1996) and *Phys. Rev.* **D57**, 4453 (1998) .
- [16] D. Choudhury and S. Raychaudhuri, *Phys. Rev.* **D56**, 1778 (1997) ; F. Abe *et al*, CDF Collaboration, Fermilab preprint FERMILAB-PUB-98-374-E (1998).
- [17] R.M. Godbole, P. Roy and X. Tata, *Nucl. Phys.* **B401**, 67 (1993) .
- [18] G. Ganis, MPI Munich preprint MPI-PHE-98-14 (1998), hep-ex/9811046; ALEPH Collaboration, R. Barate *et al.*, *Eur. Phys. J.* **C7**, 383 (1998) ; DELPHI Collaboration, R. Keranen, *Chargino, neutralino and sfermion searches (R parity) at LEP-2*, in *Barcelona 1997, Quantum effects in the minimal supersymmetric standard model* p. 345-350. L3 Collaboration, M. Acciarri *et al.*, *Phys. Lett.* **B414**, 373 (1997) ; OPAL Collaboration, G. Abbiendi *et al.*, CERN preprint CERN-EP-98-203 (1998), hep-ex/9901037;
- [19] F. Abe *et al.*, CDF Collaboration, Fermilab preprint FERMILAB-PUB-98-374-E (1998); S. Abachi *et al*, D0 Collaboration, URL: <http://www-d0.fnal.gov/public/new/analyses/rpreejjjj/welcome.html>
- [20] See, for example, J.L. Feng, *et al.*, *Phys. Rev.* **D52**, 1418 (1995) .
- [21] H. Dreiner and S. Lola, Oxford University preprint OUTP-92-02P (1992) (unpublished).
- [22] J.L. Feng, *et al.*, *Phys. Rev.* **D52**, 1418 (1995) ; J.L. Feng and D.E. Finnell, *Phys. Rev.* **D49**, 2369 (1994) ; J.A. Bagger, *Nucl. Phys. Proc. Suppl.* **62**, 23 (1998);
- [23] E. Accomando *et al.*, *Phys. Rept.* **299**, 1 (1998) and references therein.

- [24] V. Barger, M.S. Berger, P. Ohmann and R.J. Phillips, *Phys. Rev.* **D50**, 4299 (1994) ; H. Baer, C. Kao and X. Tata, *Phys. Rev.* **D51**, 2180 (1995) .
- [25] D. Choudhury, *Phys. Lett.* **B376**, 201 (1996) .
- [26] M. Chemtob and G. Moreau, *Phys. Rev.* **D59**, 055003 (1999) .
- [27] A. Bartl *et al.* , in *New Directions for High Energy Physics*, (Snowmass, 1996), p. 693; I. Hinchliffe, *et al.* , *Phys. Rev.* **D55**, 5520 (1997) .
- [28] A. Hocker, *The Status of MSSM Higgs Boson Searches at LEP*, to appear in the proceedings of the American Physical Society (APS) Meeting of the Division of Particles and Fields (DPF 99), Los Angeles, (5-9 Jan 1999), hep-ex/9903024.
- [29] H. Baer, A. Bartl, D. Karatas, W. Majerotto, and X. Tata, *Int. J. Mod. Phys.* **A4**, 4111 (1989) ; A. Bartl, H. Fraas, W. Majerotto, *Z. Phys.* **C30**, 441 (1986) , *Nucl. Phys.* **B278**, 1 (1986) and *Z. Phys.* **C34**, 411 (1987) ; see also A. Bartl, W. Majerotto and B. M \ddot{o} ßlacher in *Phenomenological Aspects of Supersymmetry*, Proceedings of a Series of Seminars Held at the Max-Planck-Institut für Physik Munich, FRG, May to November 1991, W. Hollick, R. Rückl, J. Wess (Eds.) (Springer-Verlag).
- [30] J. Kalinowski, *Acta Phys. Pol.* **B28**, 2423 (1997), hep-ph/9712550 and hep-ph/9708490 (unpublished).
- [31] V. Barger, W.-Y. Keung and R.J. Phillips, *Phys. Lett.* **B364**, 27 (1995) .
- [32] A. Bartl, H. Fraas, W. Majerotto, *Z. Phys.* **C41**, 475 (1988) .
- [33] E.A. Baltz and P. Gondolo, *Phys. Rev.* **D57**, 2969 (1998) .
- [34] L. Roszkowski, in *Waikoloa Linear Collid.* (1993) p.0854, hep-ph/9309208.
- [35] T.G. Rizzo, SLAC preprint SLAC-PUB-7982 (1998), hep-ph/9811440.
- [36] ALEPH Collaboration, R. Barate *et al.* , *Phys. Lett.* **B420**, 196 (1998) .
- [37] D.K. Ghosh and S. Raychaudhuri, *Phys. Lett.* **B422**, 187 (1997) .
- [38] D.K. Ghosh, R.M. Godbole and S. Raychaudhuri, *Z. Phys.* **C75**, 357 (1996) .

Appendix A: Decay Widths of the LSP

The decay of the LSP is mediated by R -parity-violating couplings, which arise from the superpotential of Eq. (2). In terms of component boson and fermion fields, this leads to an interaction Lagrangian for the lepton-number-violating part, which is

$$\begin{aligned} \mathcal{L}_{int} = & - \lambda_{ijk} \left[\tilde{\ell}_{Rk}^* \bar{\nu}_i^c \frac{1-\gamma_5}{2} \ell_j + \tilde{\ell}_{Lj}^* \bar{\nu}_i \frac{1+\gamma_5}{2} \ell_k + \tilde{\nu}_i^* \bar{d}_j \frac{1+\gamma_5}{2} \ell_k - (i \leftrightarrow j) \right] \\ & - \lambda'_{ijk} \left[\tilde{d}_{Rk}^* \bar{\nu}_i^c \frac{1-\gamma_5}{2} d_j + \tilde{d}_{Lj}^* \bar{\nu}_i \frac{1+\gamma_5}{2} d_k + \tilde{\nu}_i^* \bar{d}_j \frac{1+\gamma_5}{2} d_k \right] \\ & \lambda'_{ijk} \left[\tilde{d}_{Rk}^* \bar{\ell}_i^c \frac{1-\gamma_5}{2} u_j + \tilde{u}_{Lj}^* \bar{\ell}_i \frac{1+\gamma_5}{2} d_k - \tilde{\ell}_{Li}^* \bar{u}_j \frac{1+\gamma_5}{2} d_k \right] + \text{H.c.} \end{aligned} \quad (7)$$

Using the first line of this interaction Lagrangian, we can now calculate the decay width of the neutralino in the case of a λ_{ijk} coupling. We present below complete formulae for the squared and spin-averaged matrix element for the process $\tilde{\chi}_1^0(P) \rightarrow \nu_i(p_i) \ell_k^+(p_k) \ell_j^-(p_j)$. The neutralino can also decay into the CPT -conjugate of the right side because it is a Majorana fermion. Thus we should include a factor of 2 when calculating the decay width.)

$$|\mathcal{M}(\tilde{\chi}_1^0 \rightarrow \nu_i \ell_k^+ \ell_j^-)|^2 = \frac{12\pi\alpha\lambda_{ijk}^2}{\sin^2\theta_W} [T_{ii} + T_{jj} + T_{kk} + T_{ij} + T_{ik} + T_{jk}] \quad (8)$$

where the terms T_{ii} etc. refer to the squares of the amplitudes containing a sfermion of flavour i in the propagator (see Fig. 8), and T_{ij} etc. are the interference terms. Similarly we denote the masses of ℓ_i^\pm by m_i , the masses of $\tilde{\ell}_i$ by \tilde{m}_i and the mass of the neutralino by M_1 . Then

$$\begin{aligned} T_{ii} &= \frac{p_j \cdot p_k}{D_i^2} [(G_{Li}^2 + G_{Ri}^2) P \cdot p_i] \\ T_{jj} &= \frac{p_i \cdot p_k}{D_j^2} [(G_{Lj}^2 + G_{Rj}^2) P \cdot p_j + 2G_{Lj} G_{Rj} M_1 m_j] \\ T_{kk} &= \frac{p_i \cdot p_j}{D_k^2} [(G_{Lk}^2 + G_{Rk}^2) P \cdot p_k + 2G_{Lk} G_{Rk} M_1 m_k] \\ T_{ij} &= \frac{-1}{D_i D_j} [G_{Li} G_{Lj} (-p_i \cdot p_j P \cdot p_k + p_i \cdot p_k P \cdot p_j + p_j \cdot p_k P \cdot p_i) + G_{Li} G_{Rj} M_1 m_j p_i \cdot p_k] \\ T_{ik} &= \frac{-\eta_1}{D_i D_k} [G_{Lj} G_{Lk} (p_i \cdot p_j P \cdot p_k - p_i \cdot p_k P \cdot p_j + p_j \cdot p_k P \cdot p_i) + G_{Li} G_{Lk} M_1 m_k p_i \cdot p_j] \\ T_{jk} &= \frac{-\eta_1}{D_j D_k} \left[G_{Lj} G_{Rk} (p_i \cdot p_j P \cdot p_k + p_i \cdot p_k P \cdot p_j - p_j \cdot p_k P \cdot p_i) \right. \\ &\quad \left. + G_{Lj} G_{Rk} m_j m_k P \cdot p_i + G_{Rj} G_{Lk} M_1 m_k p_i \cdot p_j + G_{Rj} G_{Rk} M_1 m_j p_i \cdot p_k \right] \end{aligned} \quad (9)$$

where $D_{i,j,k} = (s_{i,j,k} - \tilde{m}_{i,j,k}^2)$, $s_{i,j,k} = (P - p_{i,j,k})^2$, η_1 is the sign of the mass eigenvalue of the lightest neutralino, and the couplings G_{Li}, G_{Ri} etc. are defined by the interaction of the neutralino with a lepton–slepton pair:

$$\mathcal{L}_{int} = -\frac{g}{2\sqrt{2}} \{ (1 + \eta_1) + i(1 - \eta_1) \} \tilde{\chi}_i^0 \left\{ G_{Ln} \frac{1-\gamma_5}{2} + G_{Rn} \frac{1+\gamma_5}{2} \right\} \ell_n \tilde{\ell}_n^* + \text{H.c.} \quad (10)$$

The non-vanishing chiral couplings which enter into the above matrix element are given by

$$\begin{aligned}
G_{Li} &= \eta_1(N_{12} - N_{11} \tan \theta_W), \\
G_{Lj} &= -\eta_1(N_{12} + N_{11} \tan \theta_W), \\
G_{Rj} &= m_j N_{13}/(\sqrt{2}M_W \cos \beta), \\
G_{Lk} &= \eta_1 m_k N_{13}/(\sqrt{2}M_W \cos \beta), \\
G_{Rk} &= 2N_{11} \tan \theta_W,
\end{aligned} \tag{11}$$

where N is the neutralino mixing matrix (see Ref. [1]). In the above set of formulae, we note that we have not taken into account the possibility of slepton resonances in the decay of the neutralino. This is because the neutralino is considered to be the LSP throughout this article⁹. We have however, taken into account sign changes due to chiral rotations of the neutralino fields necessitated by negative mass eigenvalues.

It is trivial to translate the above set of results to the case of a λ'_{ijk} coupling, where the decay process is $\tilde{\chi}_1^0(P) \rightarrow \nu_i(p_i)d_j(p_j)\bar{d}_k(p_k)$. We simply replace the λ -coupling by the λ' -coupling and each lepton by the corresponding d -type quark. The non-vanishing couplings of the neutralino to the relevant quark–squark pairs are now given by

$$\begin{aligned}
G_{Li} &= \eta_1(N_{12} - N_{11} \tan \theta_W), \\
G_{Lj} &= -\eta_1(N_{12} - \frac{1}{3}N_{11} \tan \theta_W), \\
G_{Rj} &= m_j N_{13}/(\sqrt{2}M_W \cos \beta), \\
G_{Lk} &= \eta_1 m_k N_{13}/(\sqrt{2}M_W \cos \beta), \\
G_{Rk} &= \frac{2}{3}N_{11} \tan \theta_W.
\end{aligned} \tag{12}$$

In the other case for a λ'_{ijk} coupling, the relevant process is $\tilde{\chi}_1^0(P) \rightarrow \ell_i^-(p_i)u_j(p_j)\bar{d}_k(p_k)$. If we neglect the charged lepton mass (which is a pretty good approximation for the kind of neutralino masses discussed in this article), then one can again use the above formulae with appropriate replacements, and taking

$$\begin{aligned}
G_{Li} &= -\eta_1(N_{12} + \frac{1}{3}N_{11} \tan \theta_W), \\
G_{Ri} &= m_i N_{13}/(\sqrt{2}M_W \cos \beta), \\
G_{Lj} &= \eta_1(N_{12} + \frac{1}{3}N_{11} \tan \theta_W), \\
G_{Rj} &= m_j N_{14}/(\sqrt{2}M_W \sin \beta), \\
G_{Lk} &= \eta_1 m_k N_{13}/(\sqrt{2}M_W \cos \beta), \\
G_{Rk} &= \frac{2}{3}N_{11} \tan \theta_W.
\end{aligned} \tag{13}$$

⁹It is easy to translate the above results to the case when there are slepton resonances. We simply replace the propagators $(s_n - \tilde{m}_n^2)$ by the Breit-Wigner forms $(s_n - \tilde{m}_n^2) + i\tilde{m}_n\Gamma_n$, where Γ_n is the total decay width of the n th slepton. This decay width is easily calculated, since the slepton in question is now the LSP and will undergo a two-body decay through the R -parity-violating coupling in question.

The real difference between the cases for λ and λ' couplings arises when kinematics allows one to have a top quark in the final state, in which case it is possible to have $m_j = m_t$, which makes G_{Rj} large. However, these have not been considered in this work.

We now pass on to the case of baryon-number-violating λ'' couplings, where the interaction Lagrangian is given by

$$\mathcal{L}_{int} = - \lambda''_{ijk} \left[\tilde{d}_{Rk}^* \bar{d}_j \frac{1+\gamma_5}{2} u_i^c + \tilde{d}_{Rj}^* \bar{u}_i \frac{1-\gamma_5}{2} d_k^c + \tilde{u}_{Ri}^* \bar{d}_j^c \frac{1+\gamma_5}{2} d_k \right] + \text{H.c.} \quad (14)$$

This allows us to have the decay $\tilde{\chi}_1^0(P) \rightarrow u_i(p_i) d_j(p_j) d_k(p_k)$ together with the CPT -conjugate of the right side. Using the same kind of convention as in the case of lepton-number-violating operators, the matrix element, squared and summed over spins, has the form

$$|\mathcal{M}(\tilde{\chi}_1^0 \rightarrow u_i d_j d_k)|^2 = \frac{24\pi\alpha\lambda''_{ijk}{}^2}{\sin^2\theta_W} [T_{ii} + T_{jj} + T_{kk} + T_{ij} + T_{ik} + T_{jk}] \quad (15)$$

where

$$\begin{aligned} T_{ii} &= \frac{p_j \cdot p_k}{D_i^2} \left[(G_{Li}^2 + G_{Ri}^2) P \cdot p_i + 2G_{Li} G_{Ri} M_1 m_i \right] \\ T_{jj} &= \frac{p_i \cdot p_k}{D_j^2} \left[(G_{Lj}^2 + G_{Rj}^2) P \cdot p_j + 2G_{Lj} G_{Rj} M_1 m_j \right] \\ T_{kk} &= \frac{p_i \cdot p_j}{D_k^2} \left[(G_{Lk}^2 + G_{Rk}^2) P \cdot p_k + 2G_{Lk} G_{Rk} M_1 m_k \right] \\ T_{ij} &= \frac{-1}{D_i D_j} \left[G_{Ri} G_{Rj} (-p_i \cdot p_j P \cdot p_k + p_i \cdot p_k P \cdot p_j + p_j \cdot p_k P \cdot p_i) \right. \\ &\quad \left. + G_{Li} G_{Lj} m_i m_j P \cdot p_k + G_{Li} G_{Rj} M_1 m_i p_j \cdot p_k + G_{Ri} G_{Lj} M_1 m_j p_i \cdot p_k \right] \\ T_{ik} &= \frac{-\eta_1}{D_i D_k} \left[G_{Ri} G_{Rk} (p_i \cdot p_j P \cdot p_k - p_i \cdot p_k P \cdot p_j + p_j \cdot p_k P \cdot p_i) \right. \\ &\quad \left. + G_{Li} G_{Lk} m_i m_k P \cdot p_i + G_{Li} G_{Rk} M_1 m_i p_j \cdot p_k + G_{Ri} G_{Lk} M_1 m_k p_i \cdot p_j \right] \\ T_{jk} &= \frac{-\eta_1}{D_j D_k} \left[G_{Rj} G_{Rk} (p_i \cdot p_j P \cdot p_k + p_i \cdot p_k P \cdot p_j - p_j \cdot p_k P \cdot p_i) \right. \\ &\quad \left. + G_{Lj} G_{Lk} m_j m_k P \cdot p_i + G_{Lj} G_{Rk} M_1 m_k p_i \cdot p_k + G_{Rj} G_{Lk} M_1 m_j p_i \cdot p_j \right] \end{aligned} \quad (16)$$

where we now take

$$\begin{aligned} G_{Li} &= \eta_1 m_i N_{14} / (\sqrt{2} M_W \sin \beta), \\ G_{Ri} &= -\frac{4}{3} \tan \theta_W N_{11}, \\ G_{Lj} &= \eta_1 m_j N_{13} / (\sqrt{2} M_W \cos \beta), \\ G_{Rj} &= \frac{2}{3} \tan \theta_W N_{11}, \\ G_{Lk} &= \eta_1 m_k N_{13} / (\sqrt{2} M_W \cos \beta), \\ G_{Rk} &= \frac{2}{3} \tan \theta_W N_{11}. \end{aligned} \quad (17)$$

Appendix B: The 350 GeV Option

It is, of course, feasible, and presumably planned, that a linear e^+e^- collider would first run at the $t\bar{t}$ production threshold of about 350 GeV for some time, before it actually goes on to run at 500 GeV. The situation regarding chargino and neutralino production is actually better in this case, as the dominant s -channel diagrams would be less suppressed, though of course, there would be kinematic restrictions. The signals discussed in this article can then be studied at this energy as well. However, the SM backgrounds are also enhanced considerably. This is illustrated in Table 6, where we have presented the analogues of Tables 3–5, for the point (A) in the parameter space. A glance at the table will reveal that multi-lepton signals from λ couplings will be trivially discernible over background, though one and two-lepton signals will not. For the other two cases, the signals are also quite promising.

	Coupling	$\tilde{\chi}_1^0\tilde{\chi}_1^0$	$\tilde{\chi}_1^0\tilde{\chi}_2^0$	$\tilde{\chi}_2^0\tilde{\chi}_2^0$	$\tilde{\chi}_1^+\tilde{\chi}_1^-$	Total Signal (fb)	Background fb
λ	$1\ell + \cancel{E}_T$	3.4	1.3	0.3	3.7	8.7	12929.4
	$2\ell + \cancel{E}_T$	36.1	11.4	3.0	34.9	85.4	3356.8
	$3\ell + \cancel{E}_T$	160.8	40.9	9.3	121.2	332.2	0.5
	$4\ell + \cancel{E}_T$	254.8	64.1	16.5	189.1	524.5	0.1
	$5\ell + \cancel{E}_T$	0.0	51.9	21.0	115.3	188.2	–
	$6\ell + \cancel{E}_T$	0.0	39.4	19.4	23.7	82.5	–
	$7\ell + \cancel{E}_T$	0.0	0.0	11.0	0.0	11.0	–
	$8\ell + \cancel{E}_T$	0.0	0.0	5.3	0.0	5.3	–
λ'	$1\ell + \text{jets}$	224.5	58.7	12.3	165.6	461.1	12929.4
	$2\ell + \text{jets}$	76.5	61.1	20.0	172.4	330.0	283.6
	$3\ell + \text{jets}$	0.0	46.6	26.6	70.6	143.8	0.5
	$4\ell + \text{jets}$	0.0	13.0	16.1	10.2	39.3	–
	$5\ell + \text{jets}$	0.0	0.0	8.5	0.0	8.5	–
	$6\ell + \text{jets}$	0.0	0.0	1.9	0.0	1.9	–
λ''	$1\ell + \text{jets}$	0.0	55.3	19.8	205.1	280.2	12929.4
	$2\ell + \text{jets}$	0.0	61.4	27.5	43.5	132.4	283.6
	$3\ell + \text{jets}$	0.0	0.0	14.6	0.0	14.6	0.5
	$4\ell + \text{jets}$	0.0	0.0	7.5	0.0	7.5	–

Table 6. *Illustrating the contribution (in fb) of different (light) chargino and neutralino production modes to multi-lepton signals at the NLC in the case of λ, λ' and λ'' couplings for a linear collider running at $\sqrt{s} = 350$ GeV. The point (A) in the parameter space has been chosen.*

One interesting feature of a run at 350 GeV will be that the background from $t\bar{t}$ production will be highly suppressed. As a result, the invariant mass construction used in Fig. 12 would probably be more certain to yield signals distinguishable above background. Apart from this, there does not seem to be any major advantage, from the point of view of studying R -parity-violation, of a run at $\sqrt{s} = 350$ GeV.

Appendix C: Standard Model Backgrounds to Multilepton Signals

In order to obtain Standard Model backgrounds to the multi-lepton signals discussed in the text, we have considered several processes listed in Tables 7 and 8. These include $2 \rightarrow 2$ processes like $e^+e^- \rightarrow W^+W^-$, $e^+e^- \rightarrow ZZ$ and $e^+e^- \rightarrow t\bar{t}$, and a host of $2 \rightarrow 3$ processes. These were evaluated using the MadGraph package and the cross-sections were calculated using a parton-level Monte Carlo generator. The cuts mentioned in Section 4 were applied and the results were convoluted with the appropriate leptonic and hadronic branching ratios of the W and Z bosons.

In Table 7, we present a list of the contributions to the multi-lepton plus missing (transverse) energy states from various SM processes. For these, we require a minimum of 20 GeV for the \cancel{E}_T (see Section 4) and this essentially means that only processes which have a hard neutrino in the final state need be considered. In the third row of this table, we have added contributions from $e^+e^- \rightarrow t\bar{t}g$ to those from $e^+e^- \rightarrow t\bar{t}$, since the final states will be very similar, except for jet multiplicity. This increases the cross-section by about 10%.

It is also important to point out that we have included only processes which have cross-sections greater than 1 fb (before convoluting with branching ratios). For this reason, we have not considered processes like $e^+e^- \rightarrow t\bar{t}Z$ and $e^+e^- \rightarrow ZZZ$, which could also, in principle, yield multi-lepton final states.

Process	$\ell^\pm + \cancel{E}_T$	$\ell^+\ell^- + \cancel{E}_T$	$3\ell + \cancel{E}_T$	$4\ell + \cancel{E}_T$
$e^+e^- \rightarrow W^+W^-$	2361.4 (4250.5)	560.7 (1009.3)	–	–
$e^+e^- \rightarrow ZZ$	–	13.6 (23.1)	–	–
$e^+e^- \rightarrow t\bar{t} (g)$	233.7 (0.0)	55.5 (0.0)	–	–
$e^+e^- \rightarrow W^+W^-Z$	13.6 (4.5)	3.2 (1.0)	1.5 (0.5)	0.4 (0.1)
$e^+e^- \rightarrow e^+e^-Z$	–	11.6 (14.1)	–	–
$e^+e^- \rightarrow \ell^+\ell^-Z$	–	9.2 (15.2)	–	–
$e^+e^- \rightarrow e^+\nu_e W^- + e^-\bar{\nu}_e W^+$	1564.0 (1876.8)	743.2 (891.8)	–	–
$e^+e^- \rightarrow \ell^+\nu_\ell W^- + \ell^-\bar{\nu}_\ell W^+$	1940.0 (2910.0)	921.4 (1382.1)	–	–
$e^+e^- \rightarrow \nu_e\bar{\nu}_e Z$	–	24.6 (13.3)	–	–
$e^+e^- \rightarrow \nu_\ell\bar{\nu}_\ell Z$	–	4.4 (6.9)	–	–
$e^+e^- \rightarrow u\bar{d}W^- + \bar{u}dW^+$	2159.8 (3887.6)	–	–	–
Total	8272.5 (12929.4)	2347.4 (3356.8)	1.5 (0.5)	0.4 (0.1)

Table 7. Illustrating the contribution (in fb) of different SM processes to multi-lepton final states relevant for the NLC, running at 500 (350) GeV in the case of λ couplings. In the 6th, 8th and 10th row, $\ell = \mu, \tau$. In the last row, the contribution is summed over the first two generations.

It is clear that the only signal which can really contribute to final states with > 2 leptons and \cancel{E}_T is $e^+e^- \rightarrow W^+W^-Z$, and this has a rather small cross-section. This is the real reason why the signals from λ couplings are so striking.

In Table 8, we present a similar list of processes which lead to signals with multi-leptons and jets. In this case, we do not put any cut on the missing energy, but we require the final state to have a minimum of two jets.

Process	$\ell^\pm + \text{jets}$	$\ell^+\ell^- + \text{jets}$	$3\ell + \text{jets}$
$e^+e^- \rightarrow W^+W^-$	2361.4 (4250.5)	–	–
$e^+e^- \rightarrow ZZ$	–	47.6 (80.9)	–
$e^+e^- \rightarrow t\bar{t} (g)$	233.7 (0.0)	55.5 (0.0)	–
$e^+e^- \rightarrow W^+W^-Z$	13.6 (4.5)	4.0 (1.3)	1.5 (0.5)
$e^+e^- \rightarrow e^+e^-Z$	–	82.0 (100.0)	–
$e^+e^- \rightarrow \ell^+\ell^-Z$	–	32.2 (53.4)	–
$e^+e^- \rightarrow e^+\nu_e W^- + e^-\bar{\nu}_e W^+$	1564.0 (1876.8)	–	–
$e^+e^- \rightarrow \ell^+\nu_\ell W^- + \ell^-\bar{\nu}_\ell W^+$	1940.0 (2910.0)	–	–
$e^+e^- \rightarrow u\bar{d}W^- + \bar{u}dW^+$	2159.8 (3887.6)	–	–
$e^+e^- \rightarrow q\bar{q}Z$	–	21.8 (48.0)	–
Total	8262.5 (12929.4)	243.1 (283.6)	1.5 (0.5)

Table 8. Illustrating the contribution (in fb) of different SM processes to multi-lepton final states relevant for the NLC, running at 500 (350) GeV in the case of λ' and λ'' couplings. In the 6th and 8th row, $\ell = \mu, \tau$, while in the 9th row, the contribution is summed over the first two generations. In the last row, the flavour sum is carried over all quarks except the t -quark.

As before, the only process which leads to > 2 leptons in the final state is $e^+e^- \rightarrow W^+W^-Z$, and this has a very small cross section. The single-lepton plus jets and dilepton plus jets final states, however, which form the major signals for R -parity-violation with λ' and λ'' couplings, have large backgrounds. Most of these come from final states with W bosons, and hence, the removal of states where jet-pairs reconstruct to W -bosons could be a useful technique for background reduction.

Finally, we comment on effects of initial-state radiation (ISR) on the processes under consideration. The signals for chargino and neutralino production arise essentially from s -channel processes and, as such, would be enhanced by ISR effects, even though these effects are rather small. Many of the backgrounds, however, are essentially t -channel effects and these would be suppressed rather than enhanced by ISR. We thus feel that our analysis, which neglects ISR effects, is a conservative one.